COVID-19: Attacks the 1-Beta Chain of Hemoglobin to Disrupt Respiratory Function and Escape Immunity by Capsid-Like System

Wenzhong Liu[1,2,*], Hualan Li[2]

[1] School of Computer Science and Engineering, Sichuan University of Science & Engineering, Zigong, 643002, China;
[2] School of Life Science and Food Engineering, Yibin University, Yibin, 644000, China;
[*]Correspondence.Wenzhong Liu, liuwz@suse.edu.cn.

Abstract

The genetic recombination of the SARs-CoV-2 virus in bats may result in behaviors comparable to those of certain RNA viruses. This cross-activity helps explain SARs-CoV-2's strange respiratory symptoms and immune evasion abilities. In this present study, the biological roles of SARs-CoV-2 proteins were investigated utilizing bioinformatic techniques involving the search for conserved domains. According to the study, the S and ORF3a proteins of SARs-CoV-2 possess picornavirus/calicivirus capsid domains, can bind hemoglobin, heme, and porphyrin. Both Arg134 of ORF3a and Cys44 of E are iron-binding sites for heme. The ORF3a protein has a region that converts heme into iron and porphyrin. In addition to chitin and polyphenol binding domains, the S protein also contains hemocyanin and phenoloxidase-like domains. The S protein constructs Fe-polyphenol complexes to link the red blood cell membrane, allowing SARs-CoV-2 to hitch a ride on red blood cells for fast delivery to target organs. This type of capsid-like vector delays the immune system but does not significantly alter the function of red blood cells to transport oxygen. Due to the distortion of the cell membrane, red blood cells with an excess of viral particles release hemoglobin to harm the virus. The wbl domains of the S protein respond to nitration, and then phenoloxidase domains oxidize polyphenols, allowing the virus to shed from the red blood cell membrane. ORF3a also attack 1-beta chain of hemoglobin; however, the majority of hemoglobin may retain its native structure. Patients will have variable degrees of respiratory distress and coagulation symptoms, but the hemocyanin domains of the S protein can improve a patient's respiratory status by transporting oxygen.

Keywords: Porphyrin; Heme; Hemocyanin; Phenoloxidase; Fe-polyphenol complex; immune delay

1. Background

Early COVID-19 patients manifest diarrhea[1, 2], hypotension[3] , and electrolyte abnormalities[4]. Extracorporeal membrane oxygenation (ECMO) rescues critically ill patients who exhibit unusual clinical characteristics, including hypoxia, low oxygen saturation[5, 6], and high dissolved oxygen levels. Today, a large number of mutated strains of SARs-CoV-2 have emerged, with Omicron evolving into hundreds of substrains and becoming the most prevalent variant worldwide[7]. Omicron variants evolved[8] in southern African patients with chronic infection and immunodeficiency[9]. COVID-19 patients manifested respiratory infection, encephalitis[10], viral hemorrhagic fever[11], eye infection[12], kidney[13] and liver[14] damage, necrosis of hematopoietic tissue[15], etc. multisystemic and multitissue illness. This suggests that the variant strain

significantly exacerbates the unknown respiratory complications and immune evasion abilities of earlier strains.

Researchers discovered flaviviridae, adenoviridae, iridoviridae, picornaviruses, baculoviridae, and poxviridae, as well as other viruses, in bat feces[16]. The genomes of numerous RNA viruses are segmented. When a single cell is simultaneously infected with two viruses of different genotypes, individual segments may undergo rearrangement. New molecular and immunological bases allow viruses to cross species boundaries and establish themselves in novel ecological niches[17]. Through genetic cross-recombination in bats, the original SARs-CoV-2 virus may have similar pathogenic functions to these viruses, such as a vector delivery strategy based on the capsid protein. Coronaviruses are promising virus vectors for vaccine development and, possibly, for gene therapy[18]，also proven to be a stable carrier[19].

Vector delivery strategy (that is, riding on blood cells and immune cells—the "commuter car") is a major "immune system loophole" discovered in human evolution. Viral capsids are advantageous platforms for constructing novel nanomaterials, such as hybrid structures that combine biological macromolecules and inorganic complexes. Polyphenols such as tannins modify biomolecules, including adeno-associated virus (AAV), and facilitate their association with the surface of cells (e.g., erythrocytes, macrophages, NK cells, T cells), in the presence of iron combined with[20]. On the cell surface, biologically active nanocomplexes, including proteins, DNA, mRNA, and even viral vectors, can be assembled through interfacial interactions mediated by metal (Fe3+)-phenol coordination. Frequently, polyphenols exert multiple types of stabilizing attractions[21]. Different interactions and bonding of natural polyphenols (e.g., hydrogen, π, hydrophobic, metal coordination, covalent, and electrostatic) can be utilized to assemble and stabilize polyphenol-based particles[22].

Red blood cells (RBC) anchor AAV to form RBC-AAV, which provides less than a minute of protection against nAb antibodies in the blood until deposited in the target organ of interest[23]. The Fe(III)/TA (tannic acid) coating on red blood cells (RBCs) creates immune-camouflaged RBCs while also maintaining oxygen transport[24]. The network on the cell surface does not inhibit cell receptors and molecular exchangeability, and the release kinetics can be fine-tuned by selecting different metal ions (Fe3+, Al3+, or Cu2+)[25]. Numerous viral vectors, including picornaviruses and hepatitis viruses, have been identified recently. Using adenoviral (Ad) vectors and an "antigen capsid incorporation" strategy, HIV-1 vaccines have been developed[26].

The viral S protein of SARs-CoV-2 had evolved a capsid-like activity, and it required the "commuter car" of blood cells (or immune cells) to reach its target organ. As a biosorbent, chitin can absorb phenol[27] or polyphenols from water. Some polyhedrosis viruses in baculoviruses have a chitin-binding function and are localized in the endoplasmic reticulum of insect cells by chitinase[28]. The S protein of SARs-CoV-2 contained chitin-binding domains, which adsorbed polyphenols via chitin. The S protein was connected to the red blood cell membrane via the Fe-polyphenol complex. SARs-CoV-2 was rapidly shed after reaching the target organ due to the phenoloxidase activity of S proteins oxidizing polyphenols.

Red blood cells capture viruses to counter the vector delivery strategy by creating "bait red blood cells"[29]. Red blood cells (RBCs) from nuclear rainbow trout can degrade hemorrhagic septicemia virus (VHSV)[30]. When enhanced reovirus binds to red blood cells in high concentrations, it penetrates the cell membrane, causing the red blood cells to release hemoglobin and subsequently undergo hemolysis[31]. Due to the inherent cytotoxicity of cell-free hemoglobin

(Hb), activated Hb fragments are anchored to microorganisms, while the juxtaposed pseudoperoxidase (POX) is released immediately and induces oxidative shock, thereby killing nearby pathogens[32]. Hemoglobin inhibits viral growth and replication mediated by African swine fever virus (CSFV) capsod protein by interacting with RIG-I[33]. The subunit of hemoglobin interacts with the capsid, RdRp, and VPg proteins to inhibit the replication of the rabbit hemorrhagic disease virus[34]. Hemoglobin A (HbA) contains an N-terminal fructosyl valine on its beta chain, and the lectin from Aleuria aurantia (AAL) has a greater affinity for HbA than for Hb[35]. Through the erythrocyte receptor, erythrocytic protein and glycophorin inhibit the hemagglutination of rhesus monkey rotavirus (RRV) [36].

Hemoglobin's heme component is toxic. Hemoglobin's heme activates human and mouse platelets via C-type lectin-like receptor 2[37]. Human heme and HO-1 inhibit hepatitis C virus, human immunodeficiency virus, and hepatitis B virus replication[38]. Heme and related compounds exhibit striking similarity at viral target sites in all three species[38]. Dengue (DENV), Yellow Fever (YFV), Chikungunya (CHIKV), and Zika (ZIKA) virus, Mayaro virus, Sindbis virus, and vesicular stomatitis virus infectious particles are all inactivated by heme, Cobalt Protoporphyrin IX (CoPPIX), and Sn-Protoporphyrin IX (SnPPIX)[39]. In addition, photostimulation improved the efficacy of SnPPIX against all arboviruses tested[39].

The native neuronecrosis virus capsid protein (NNVCP) binds hemoglobin and transferrin, causing anemia in grouper fish[40]. The CSFV capsid protein inhibits hemoglobin action by interacting with the -subunit[33]. In children, parvovirus B19 invading erythroid precursor cells in the bone marrow causes pure red cell aplasia (PRCA) and rash[41]. The erythrocytic necrosis virus (ENV, Iridoviridae) causes viral nuclear necrosis (VEN) in marine and anadromous fish[42]. Numerous salmonid-infected erythrocytes contain viral inclusions in their cytoplasm[43]. The virus was also detected in the erythrocytes of rainbow trout (Salmo gairdneri) that had been infected[44]. Piscine orthoreovirus, the agent responsible for heart and skeletal muscle inflammation (HSMI) in Atlantic salmon, has also been linked to erythrocytes with cytoplasmic inclusions[45]. Positive nuclear staining of erythrocytes in the hepatic sinusoidal space of chickens infected with the novel duck reovirus (NDRV) indicated the presence of viral protein antigens[46]. Infected blood cells (blue), neurons, and fat body cells contain cytoplasmic aggregates of iridescent Armadillidium vulgare virions[47]. Notably, Armadillidium vulgare blood cells contain hemocyanin, not hemoglobin.

In general, viral attacks on hemoglobin should lead to a pronounced hypoxic state in the body. Ground-glass images are frequently linked with severe hypoxia. Despite significant hypoxemia, some individuals with COVID-19 pneumonia experience no dyspnea, demonstrating the "happy hypoxia" paradox. Altitude sickness' physiological characteristics and symptoms at high altitude are comparable to those of various illnesses related to COVID-19[48]. The SARs-CoV-2 virus may contain a hemocyanin-like protein that binds oxygen and activates the phenoloxidase activity of the virus. Hemocyanin-mediated oxygenation leads to effective O2 transport under hypoxic settings[49]. COVID-19 patients had hemoglobin and hemocyanin-like co-transport oxygen patterns. In this mode, oxygen supplied by hemocyanin-like molecules compensates for bodily hypoxia even when red blood cells or hemoglobin were not working adequately. Thus, when viruses attacked hemoglobin, it exhibited “high dissolved oxygen”. In contrast, hemocyanin-like proteins exhibited an abnormal oxygen transport function, resulting in "happy hypoxia."

Hemocyanin comprises three domains[50]: a N-terminal domain, an active site containing

binuclear copper ions, and a C-terminal domain[51]. Conformational changes in the N-terminal domain can activate hemocyanin's phenoloxidase activity. The C-terminal domain contributes to organisms' immunological agglutination activity[52] and increases blood cell phagocytosis[53]. Hemocyanin is found only in hemolymph and appears in hexamers or hexameric oligomers[54]. The active site catalyzes the chelation of two copper ions and the binding of an oxygen molecule [55]. Hemocyanin is more than twice the size of hemoglobin[56]. Hemocyanin reversibly binds to oxygen molecules via altering the valence of copper ions（Cu^{2+}↔Cu+）[57]. It binds 96 oxygen molecules, whereas hemoglobin only binds four[56].

Hemocyanin molecules float freely in the blood, whereas red blood cells contain millions of smaller hemoglobin molecules[56]. Hemocyanin and hemoglobin have complementary distributions in some insect orders[58] and crustaceans[59]. Hemocyanin and hemoglobin are both present in the crustaceans, Hymenoptera and Hemiptera. Hemocyanin works as a physiological supplement, compensating for poor oxygen transport in the trachea and assisting insect embryos in aerobic respiration[60]. Hemocyanin expression was dramatically increased in Baifutiao[61] and locust embryos[62] under hypoxia conditions compared to normoxic settings. Increased hemocyanin content assists locust embryos in obtaining adequate and steady oxygen in hypoxic high altitude locations[62]. Hemocyanin expression was also significantly elevated in the blue crab Callinectes sapidus [63] and the ecliptic crab Cancer magister[64] under hypoxic conditions [65].

Hemocyanin is homologous to phenoloxidases such as tyrosinase because both proteins have a type 3 Cu active site coordination[66]. Enzymes of phenoloxidase (PO), such as tyrosinase and catechol oxidase Catecholamine (CA) is a catechol derivative. The enzymatic reaction catalyzed by phenoloxidase results in chromogen, melanin, and other pigments[67]. The phenoloxidase(PO) enzymes significantly contribute to hyperpigmentation[68]. Insect prophenoloxidase (PPO) is also an important innate immune protein as it is involved in cellular and humoral defenses[69]. Tyrosine hydroxylase can convert tyrosine to o-diphenols, whereas phenoloxidase can convert o-diphenols to quinones[70]. The phenoloxidases of perennial plants have hydroxylase activity[71]. In a pH-dependent manner, the heme-phage (capsid) complex oxidizes a variety of peroxidase substrates, including the catechol derivative di-tert-butylcatechol[72]. In order to detach the virus from the red blood cell membrane, the S protein with capsid activity oxidized polyphenols through phenoloxidase activity.

Using a cysteine-rich region, the SARs-CoV spike protein (S) and ORF3a form an interchain disulfide bond on the inside of the viral envelope[73]. Co-mutation trends are proven by the disulfide bond between the ORF3a protein and the spike protein of SARs-CoV. Cysteine residues are also associated with the homodimerization of the SARs-CoV ORF3a protein[74]. The homodimer is conserved in all viruses[74], including SARs-CoV-2. ORF3a of SARs-CoV-2 resides in the plasma membrane, where it forms Ca2+ ion channels[75]. Or insert within the viral envelope and interact with the S protein to promote viral uptake[75]. The S Q57H mutation affects the interaction between the ORF3a-S and ORF3a-ORF8 proteins[76]. When the SARs S protein detected the threat of NO nitration, conformational changes caused S to break the disulfide bond and release ORF3a to bind Hb or Heme. However, corresponding to the cysteine-rich region of SARs ORF3a, SARs-CoV-2 ORF3a exhibits a degree of mutation. On the SARs-CoV-2 virus, no direct evidence of the formation of a stable S-ORF3a complex via disulfide bonds was discovered. As a result, ORF3a evolved into a protein that constantly monitored threat signals emitted by hemoglobin and nitrogen free radicals.

The SARs-CoV-2 ORF3a protein also has an extremely similar function included 催化活性 to that of the capsid protein. Significant CD4+ and CD8+ T cell responses against ORF3a were observed in SARs-CoV-2-infected individuals[77]. ORF3a triggers substantial CD4+ and CD8+T cell responses[78]. More healthy adults have a higher frequency of circulating AAV capsid-specific CD8 and/or CD4+ T cells, T cell-mediated immune responses to AAV, and AAV vectors[79]. ORF3a of SARs-CoV-2 enhances viral export by means of lysosomal exocytosis[80]. induce a secondary infection[81]. SARs-CoV-2 ORF3a protein inhibits IFN signaling to effectively evade host immune responses[82]. Six different flavivirus capsid proteins inhibit the expression of type I interferon and interferon-stimulated genes[83].

SARs-CoV-2 ORF3a associates with early and late endosomes and lysosomes to promote endocytosis[75]. The YXX motif of SARS and SARs-CoV-2 ORF3a facilitates host contact[84]. The minor capsid protein L2 of human papillomavirus (HPV) types contains multiple Yxx sorting signals to varying degrees. Vesicle protection facilitates the sorting and transport of endocytic cargo[85]. The YXX motif plays a crucial role in the events that follow clathrin-free cleavage. Likewise, it affects the HCV life cycle by boosting viral replication[86]. The YXX[I/L/M/F/V] motif and YXX-like tetrapeptide confer specific functions, such as virulence, host immunity regulation, and pathogenesis, to the nucleocapsid protein of Hantavirus[87]. HCV virions assemble on or near the surface of lipid droplets and acquire an envelope core at the endoplasmic reticulum (ER), where the YXX motif mediates the recruitment of the AP-2 complex subunit mu (AP2M1) to lipid droplets[88]. HCV capsid assembly is independent of signal sequence cleavage and depends on the N-terminus of the HCV core rather than the C-terminus[89].

ORF3a's capsid-like activity is a "killer weapon" used by viruses to deceive and attack. Capsid protein has the ability to bind porphyrin and exert catalytic activity. The inner surface of the self-assembled spherical phage MS2 capsid was modified with up to 180 porphyrins capable of producing toxic singlet oxygen, which killed a significant number of Jurkat cells when exposed to light[90]. The potential iron-binding ligand structure of the hepatitis B virus (HBV) capsid protein was genetically modified with multivalent metallo-porphyrin (such as heme) modifications[91]. The core particle of HBV is internalized by clathrin-mediated endocytosis, resulting in lysosomal cleavage of the core monomer and particle dissociation[85].

ORF3a targeted hemoglobin and heme, much like the proteins of certain bacterial pathogens. Pathogenic *E. coli* strains can use hemoglobin as a source of iron[92]. Hemoglobin protease (Hbp) is a proteolytic enzyme similar to IgA1 protease. The immunoglobulin A1 protease (IgA1 protease) is a serine protease (S6 family) that is produced by several pathogenic bacteria[93], colonizing human mucosal surfaces, affecting specific immune responses[93]. This serine protease autotransporter, released from *E.coli*, destroys hemoglobin, binds the liberated heme, and transports it to both bacteria[94].

When *Staphylococcus aureus*'s Isd protein degrades hemoglobin, the 1-beta chain is targeted first, releasing heme and initiating a series of heme release events. Heme transfer from met-Hb to IsdH/B is slower than from met-Hb to full-length Hb receptors[95]. It is also governed by simple heme dissociation from met-Hb[96]. By binding to αHb via the IsdH or IsdB domains, the rate of efficient interactions between the Hb chain and the heme receptor domain is increased[97]. This binding is used to specifically target the heme receptor domain, regulating the sequential release of heme from βHb and αHb chains[97]. The αHb·βHb dimer releases heme from a single subunit (half-Hb) while retaining the majority of its natural structure[98]. It remains linked with the Hb

receptor until all heme is released. IsdH does not bind to free apo-Hb. The IsdH-Hb complex dissociates only when the heme in Hb is completely removed[97].

The ORF3a protein may interact with αHb via the Isd domains and then break βHb using the IgA1 protease structure.It is possible that the Isd domains overlap with the capsid domain. This attack on the 1-beta chain of hemoglobin initiated the sequential release of heme from hemoglobin. The IsdC protein from *S. aureus* uses a flexible binding pocket to capture heme[99]. The crystal structure of the heme-IsdC complex is the central conduit of the *S. aureus* Isd iron/heme uptake system[100]. IsdA , IsdB, IsdH, and IsdC share the same heme-binding module, termed the NEAT (near transporter) domain[100]. However, it is possible that the iron-regulated surface proteins IsdA, IsdB, and IsdH are not required for heme iron utilization in *S. aureuss*[101].

Heme iron is most frequently liberated from heme's oxidative breakdown by heme oxygenase (HO). Most of the time, iron is released from heme due to the protoporphyrin ring degrading[102]. *C. diphtheriae*'s heme oxygenase degrades heme to generate α-biliverdin, carbon monoxide, and free iron[103]. IsdG and IsdI (heme oxygenase) of *Staphylococcus aureus* cleaves the tetrapyrrole ring structure of heme in the presence of NADPH cytochrome P450 reductase, thereby releasing iron.[104]. However, *E.coli*'s deferrochelating activity does not destroy the tetrapyrrole backbone[105]. It is the case with *Yersinia enterocolitis* HemS[106] and *E. coli* O157:H7 ChuS[107] . HemS is used by *E. coli* Bartonella hensii to deal with oxidative stress caused by H_2O_2[108]. Iron is released from heme by the HemS of *E. coli* Bartonella henii without causing damage to the tetrapyrrole backbone[108]. HemS protein also degrades heme in the presence of electron donors, ascorbate, or NADPH-cytochrome P450 reductase[108]. It is possible that HemS overlaps with the capsid domain of SARs-CoV-2 ORF3a.

In this current work, we employ a conserved domain search approach to study SARs-CoV-2 viral proteins. The results showed that SARs-CoV-2 S and ORF3a proteins have picornavirus/calicivirus capsid domains in them that can bind hemoglobin, heme, and porphyrin. The S protein also has chitin binding and polyphenol binding, hemocyanin, and phenoloxidase domains. Arg134 of ORF3a and Cys44 of E are the heme iron binding sites. The ORF3a protein has a domain that breaks down captured heme into iron and porphyrin. SARs-CoV-2 ORF3a proteins have the ability to target 1 beta-chain of hemoglobin and dissociate heme into iron and porphyrin.

2. Methods

2.1 Data set

1. The sequences of SARs-CoV-2 proteins. The SARs-CoV-2 protein sequences came from the NCBI database. Including: S, E, N, M, ORF3a, ORF8, ORF7a, ORF7b, ORF6, ORF10, orf1ab, orf1a. Among them, the orf1ab and orf1a sequences also included corresponding subsequences. SARs-CoV-2 variant's (Delta and Omicro) ORF3 and ORF8 sequences came from the NCBI.

2. Related sequences. The related sequence was downloaded from UniProt data set (Table 1).

Table 1. Related sequences are used to search for conserved domains

No	Related protein	Keywords	Count
1	polyphenol	phenol	103,372
		polyphenol	34,592
2	capsid	virus capsid	771,290
		Adenovirus + capsid	18,037
		Baculovirus	5,311
		parvovirus B19	4,630
		classical swine fever virus Capsid	255
		Flaviviridae Capsid	61,316
		hemorrhagic disease virus	2,979
		erythrocyte necrosis virus	228
		iridescent virus	2,359
		Poliovirus	13,668
		Orthoreovirus	4,862
		Reoviridae	6,368
3	cytochrome c	Bacterial+ cytochrome + c	111,967
4	Hemoglobin	Hemoglobin	56,870
5	Hemoglobin degrading	hemoglobin+protease;Hemoglobin+hydrolysis; hemoglobin+degrading;hemoglobin+degrade; Hemoglobin+decomposition; Hemoglobin+breakdown	2,106
6	HEME Degrade	Bacterial+heme+oxidase; ChuS;EfeB;HemS;HmuS;IsdG;MhuD;PhuS ShuS;YfeX	41,325
7	Hemocyanin	Hemocyanin;crustacean	9,780

2.2 A localized MEME tool to identify conserved domains.

The following are the steps involved in the analysis:

1. Downloaded MEME[109] from the official website and installed it in a virtual machine running Ubuntu. VM 15 was the virtual machine.

2. Downloaded the SARs-CoV-2 protein sequence from the National Center for Biotechnology Information's official website.

3. Obtained the fasta format sequences of the related protein from the official Uniprot website.

4. Generated fasta format files by MEME analysis for each sequence in all related proteins and each SARs-CoV-2 protein sequence.

5. To create multiple batches of the files generated in Step 4, a batch size of 50000 or 100000 was used. It was limitedby the virtual ubuntu system's limited storage space.

6. Using MEME tools in batches, searched for conserved domains (E-value<=0.05) in SARs-CoV-2 and related proteins in Ubuntu.

7. Collected the conserved domains' result files. Located the domain name associated with the motif in the UniProt database.

8. Analyzed the activity of each SARs-CoV-2 protein's domains.

2.3 IBS tool

With the local version of IBS tool[110], it can make diagrams of protein and nucleic acid domains, as well as signal pathways.

Set the lines and background color of the protein or nucleic acid frame to white (or the background color of the drawing board) when creating a signal pathway diagram, and the protein or nucleic acid frame will not be visible. Other components' drawing methods remain unchanged. Using a variety of shapes, lines, and text, it is nearly possible to create signal pathway diagrams.

3. RESULTS

3.1 Domains of S protein for polyphenol binding and nitrification monitoring

Chitin-binding type-2 (PS50940) is a domain that binds chitin. Type 2 is primarily found in proteins from animals and baculoviruses. class II chitinases in animals breaks down both chitin and chitotriose. It contributes to the defense against nematodes and other pathogens in mammals. The domain is extracellular. Metallophos (PF00149) are calcineurin-like phosphatases that consist of protein phosphate phosphatases, nucleotidases, sphingomyelin phosphodiesterases, and 2'-3' cAMP phosphodiesterases and nucleases.

4Fe-4S Wbl-type (PS51674) is an iron-sulfur binding domain profile of the 4Fe-4S-like WhiB (Wbl) type. The presence or absence of [4Fe-4S] clustering, as well as its state (nitrosylated or not), are required for WBL-mediated transcriptional regulation. This class of 4Fe-4S binding proteins can be identified by the pattern of cysteine residues in the iron-sulfur region. S-nitrosation primarily functions as a transient intermediate in the formation of disulfide. Disulfide bond formation precedes observable protein S-nitrosothiol accumulation, and multiple NO donors induce protein S-thiolation[111]. Hemoglobin and heme are primarily toxic to viruses due to the NOS and RNS produced by nitrification and oxidation, respectively. The ability of human norovirus GII.4 to bind tissue blood group antigens is altered by the presence of free chlorine and peroxynitrite[112]. WhiB1 is a NO-responsive Wbl protein (Actinomyces iron-sulfur protein), and nitrosylation of the iron-sulfur cluster permits positively charged residues in the C-terminal helix to participate in DNA binding[113]. Mycobacterium tuberculosis WhiB1's [4Fe-4S] cluster is relatively insensitive to oxygen but extremely sensitive to nitric oxide (NO)[114]. A WhiB-like protein containing [4Fe-4S] is a regulatory switch of actinomycetes in response to superoxide, disulfide, and hypoxic stress induced by lung phagocytes[115].

PPO1 KFDV (PF12143) is a polyphenol oxidase found in plants and plastids. PPO1 DWL (PF12142) is an intermediate domain of polyphenol oxidase. Sulfotransfer 1 (IPR000863) contains the phenol sulfate phenol sulfotransferase domain. These enzymes are responsible for the transfer of sulfate groups into particular molecules.

Sulfatase (IPR000917) is a sulfonase, an enzyme that catalyzes the hydrolysis of diverse sulfate esters. Sulf transp (IPR007272) is a sulfur transport domain involved in the transport of molecules containing sulfur.

Using the MEME native tool, we compared polyphenol-associated proteins and capsid-associated proteins to S separately. The results of the search are shown in Table 2. The S protein contains the metallophos, PPO1, KFDV, sulfatase, and sulfotransfer 1 domains. Chitin-binding type-2, 4Fe-4S Wbl-type, PPO1 DWL, and Sulf translocation domains are also present in S proteins. There is an overlap between 4Fe-4S Wbl-type A of S, chitin-binding type-2

A, metallophos A, PPO1 KFDVA, and sulfotransfer 1 A. The 4Fe-4S Wbl-type B-C, chitin-binding type-2 B-C, Metallophos B, PPO1 DWL A, PPO1 KFDV B, Sulfatase A, and Sulfotransfer 1 B of S all overlap.

S protein Chitin-binding type-2 comes from Q6VTN5 (Choristoneura fumiferana defective polyhedrosis virus), I7B5N5 (Bombyx mandarina nucleopolyhedrovirus S2), and S5N343 (Hemileuca sp. nucleopolyhedrovirus) proteins. S The chitin-binding type-2 domain binds chitin. Tannins and other oxidized polyphenols are adsorbed by chitin. Therefore, it is capable of removing tannins, with the strongest removal ability between pH 3 and 7. Salt can stimulate it, whereas sucrose and alcohol can inhibit it. The quantity of chitin added is not proportional to the rate of tannin removal. Their distinct positions suggest that S exerts distinct effects on the adsorption of polyphenols by chitin-binding type 2. The protein S Chitin-binding protein type-2 The S1 protein contains a motif, so the bound chitin absorbs polyphenols such as tannins and is used to construct the virus vector. Polyphenols are crucial molecules that mediate the formation of capsid carriers, such as S proteins.

Table 2. Polyphenol binding and nitration monitoring domains of S protein

Protein	Domain	Alias	Motif	Start	End
S	4Fe-4S Wbl-type	A	CNDPFLGVYYHKNNKSWMESEFRVYSSANNCT FEYVSQPFLMD	136	178
		B	WPWYIW	1212	1217
		C	MVTIMLCCMTSCC	1229	1241
	Chitin-binding type-2	A	YYHKNNKSWMESE	144	156
		B	VDFCGKGYH	1040	1048
		C	LGFIAGLIAIVMVTIMLCCMTSCC	1218	1241
	Metallophos	A	YYHKNNK	144	150
		B	GKYEQYIKWPWYIWLGFIAGLIAIVMVTIMLCC	1204	1236
	PPO1_DWL	A	EQYIKWPWYIW	1207	1217
	PPO1_KFDV	A	PFLGVYYHKNNKSWMESEFR	139	158
		B	EQYIKWPWYIWLGF	1207	1220
	Sulf_transp	A	WNRKRISN	353	360
	Sulfatase	A	YEQYIKWPWYIWLGFIAGLIAIVMVTIMLCCMT SCCSCLKGCCSCGSCC	1206	1254
	Sulfotransfer_1	A	YYHKNNKSWME	144	154
		B	HGVVFLHVTYVPAQEKNFTTAPAICHDGKAHFP RE	1058	1092
		C	ELGKYEQYIKWPWYIWLGFIAGLIAIVMVTIML CCMTSCCSCLKGCCSCGSCCKFDED	1202	1259

In addition, the reductive and antioxidative properties of polyphenols will decrease the disulfide bond's stability, causing the disulfide bond to assume an unstable configuration. Thus, until the disulfide bonds of S are broken, the disulfide-bonding regions of these two proteins bind polyphenols. Due to the proximity of the S chitin-binding type-2 B and S chitin-binding type-2 C motifs to the cysteine-rich region, their adsorbed polyphenols are utilized to aid in the oxidation of the disulfide bond of S in order to break the S disulfide bond. The polyphenols bound by PPO1

and KFDV A are therefore of great assistance to the vector function of S. The polyphenols bound by PPO1 and KFDV B prevented membrane fusion by affecting the disulfide bond stability of S2.

Both the S1 protein and S2 protein regions contain 4Fe-4S Wbl-type domain motifs. This suggests that these two regions have a sensory function for NO-induced nitrosation. The chitin-binding function of chitin-binding type-2 A was eliminated by nitration of S 4Fe-4S Wbl-type A. Also lost was the polyphenol-binding function of PPO1 KFDV at S1. In the S2 membrane fusion site region, S protein also possesses chitin-binding type-2, 4Fe-4S Wbl-type, Metallophos, PPO1 DWL, PPO1 KFDV, Sulfatase, and Sulfotransfer 1 activities. Through the Wbl domain, the S protein also detects the threat posed by hemoglobin and NO; the former is primarily produced by red blood cells and the latter by macrophages. S 4Fe-4S Wbl-type A nitration changes the conformation of S2, exposing the disulfide bond region that binds to chitin and absorbs polyphenols. At least some chitin can be released by a phosphate buffer[116] that is highly concentrated. The protein phosphate phosphatase activity facilitates the elution of chitin from the S protein because both S1 and S2 contain metallophos domains. The S protein that does not bind chitin is incapable of assembling a capsid-like carrier.

3.2 Capsid-like domains of proteins S and ORF3a

Adeno_hexon (PF01065) is Hexon, the major coat protein of adenoviruses. Hexon is the principal coat protein of type 2 adenovirus. Adeno_knob (PF00541) is an adenoviral fiber protein with a knob domain.Adenovirus-specific attachment is achieved by interactions between host cell receptors and the adenoviral fiber protein, which are mediated by the carboxy-terminal knob domain of the adenoviral fiber protein.

Baculo_PEP_N (IPR007600) is the N-terminal polyhedral envelope PEP protein of the baculovirus. PEP concentrates on the polyhedron's surface and is believed to be essential for the proper formation of the polyhedron's perimeter. PEP stabilizes polyhedra and safeguards them against fusion and aggregation.

Capsid_N (PF16903) is the N-terminal domain of the major capsid protein of a variety of dsDNA viruses.

Calici_coat (PF00915) is the coat protein of the rabbit hemorrhagic disease virus (RHDV)-calicivirus. The shell domain (S domain) contains the elements required for the formation of the T=3 icosahedral capsid.

Flavi_capsid (PF01003) is capsid protein C of the flavivirus; multiple copies of the C protein form the nucleocapsid containing the ssRNA molecule.

Gag_p17 (PF00540) is the p17 protein of the GAG gene (a matrix protein). Matrix proteins form icosahedral shells associated with the mature immunodeficiency virus' inner membrane. Gag-derived proteins regulate the assembly and release of virus particles as a whole, whereas matrix proteins play crucial roles in Gag stability, capsid assembly, trafficking, and budding.

Gag_p24 (IPR000721) is the nucleocapsid Gag protein p24 of retroviruses. p24 forms the inner protein layer of the nucleocapsid and performs intricately coordinated tasks during the assembly, budding, maturation, and infection phases of the viral replication cycle.

HCV_capsid (PF01543) is the capsid protein of the hepatitis C virus. Hep core N (PF08290) is the zinc-binding domain of the hepatitis B virus core protein. This viral capsid is the primary antigen.

Nepo_coat_N (IPR005306) is the N-terminal Nepovirus coat protein. Capsid proteins form pseudo-T (three icosahedral capsid structures). Nepoviruses, along with comoviruses and

picornaviruses, are classified in the picornavirus superfamily of plus-strand single-stranded RNA viruses. Pico_P2B (IPR002527) is the 2B protein of picornavirus. During the period following poliovirus infection, membrane permeability changes dramatically. 2B and 2BC proteins enhance membrane permeability. Pico_P2A (PF00947) is a protease involved in polyprotein cleavage and is the picornavirus core protein 2A. Rhv (IPR033703) is a picornavirus and calicivirus coat protein.The Picornaviridae family consists of rhinoviruses (which cause the common cold), polioviruses, hepatitis A viruses, foot-and-mouth disease viruses, and encephalomyocarditis viruses.

Table 3. Capsid-like activity-related domains of S and ORF3a proteins

Protein	Domain	Alias	Motif	Start	End
S	Adeno_hexon	A	YYHK	144	147
		B	MLCCMTSCCSCLKGCCSCGSCCKFD	1233	1257
	Adeno_knob	A	YEQYIKWPWYIW	1206	1217
	Calici_coat	A	YEQYIKWPWYIWLGFIAGLIAIVMVTIMLCCMTSCC	1206	1241
	Calici_coat_C	A	KWPWYIWL	1211	1218
	Capsid_N	A	HKNNKSWMESEFRV	146	159
		B	ESLIDLQELGKYEQYIKWPWYIWLGFIAGLIAIVMVTIMLCCMTSCCSC	1195	1243
	Capsid_NCLDV	A	EQYIKWPWYIW	1207	1217
		B	CCMTSCCSCLKGCC	1235	1248
	Flavi_capsid	A	MSFP	1050	1053
		B	KWPWYIWLGFIAGLIAIVMVTIMLCCM	1211	1237
	Gag_p17	A	YYHKNNKSWMESE	144	156
		B	YIKWPWYIW	1209	1217
	Gag_p24	A	MQMAYR	900	905
		B	EQYIKWPWYIW	1207	1217
	Gag_p24_C	A	PWYIWLGFIAGLIAIVMVTIMLCCMTSCCSCLKGCCSC	1213	1250
	HCV_capsid	A	CGKGYHLMSFPQSAPHGVVFLHVT	1043	1066
		B	DLQELGKYEQYIKWPWYIWLGFIAGLIAIVMVTIMLCCMTSCCSCLKGCCSCGSCCKF	1199	1256
	Hep_core_N	A	EQYIKWPWYI	1207	1216
		B	MVTIMLCCMTSCCSCLKGCCSC	1229	1250
	Nepo_coat_C	A	QELGKYEQYIKWPWY	1201	1215
	Nepo_coat_N	A	IKWPWYIW	1210	1217
	Parvo_coat	A	HDGKAHFPREGVFVSNGTHW	1083	1102
		B	ELGKYEQYIKWPWYIWLGFIAGLIAIVMVTIMLCCM	1202	1237
	Pico_P2A	A	MLCCMTSCCSCLKGCCSCGSCCKF	1233	1256
	Pico_P2B	A	YAWNRKR	351	357
		B	WPWYIW	1212	1217
		C	CCMTSCCSCLKGCCSCGSCCKFDEDDS	1235	1261
	Rhabdo_ncap	A	YHKNNKSWMESEFR	145	158
		B	QELGKYEQYIKWPWYIWLGFIAGLIAIVMVTIMLCCMTSCCSCLKGCCSCG	1201	1251

	Rhv	A	VYYHKNNKSWMESEFRVYS	143	161
		B	DCTMYICGD	737	745
		C	SGWTFGAGAALQIPFAMQMAYR	884	905
		D	RVDFCGKGYHLM	1039	1050
		E	CHDGKAHFPREGVFVSNGTHWFVTQRNFYE	1082	1111
		F	ESLIDLQELGKYEQYIKWPWYIWLGFIAGLIAIVMVT IMLCCMTSCCSCLKGCCSCGSCCKFDEDDSEPVLKG VKLHYT	1195	1273
	VP4_haemagglut	A	CHDGKAHFPR	1082	1091
		B	KWPWYIW	1211	1217
	Viral_coat	A	KYEQYIKWPWYIW	1205	1217
ORF3a	Adeno_hexon	A	IMRLWLCWKCRSKNPLLYDANYFLCWHTNCYDYCI	124	158
	Adeno_knob	A	FVRIIMRLWLCWKCRSKNPLLYDANYFLCWH	120	150
	Baculo_PEP_N	A	FVRIIMRLWLCWKCRSKNPLLYDANYFLC	120	148
	Calici_coat	A	RIIMRLWLCWKCRSKN	122	137
		B	YFLCWHTNCYDYCIPYN	145	161
	Capsid_N	A	FVRIIMRLWLCWKCRSKNPLLYDANYFLCWHTNCY DYCI	120	158
		B	EHDYQIGGYTEKWE	181	194
	Capsid_NCLDV	A	MRLWLCWKCRSKNP	125	138
	Parvo_coat	A	FLQSINFVRIIMRLWLCWKCRSKNPLLYDANYFLCW HTNCYDYCI	114	158
	Rhv	A	QSINFVRIIMRLWLCWKCRSKNPLLYDANYFLCWH TNCYDYCIPYN	116	161
	Viral_coat	A	MDLFMRI	1	7
		B	YFLQSINFVRIIMRLWLCWKCRSKNPLLYDANYFLC WHTNCYDYCIPYN	113	161
		C	NKIVDEPEEH	234	243
	VP4_haemagglut	A	MRLWLCWKCRSK	125	136
		B	CWHTNC	148	153

Parvo_coat is the parvovirus coat protein VP2 (PF00740), which together with VP1 forms a vesicle. VP2 contributes to the packaging of viral DNA.Rhabdovirus ncap (PF00945) is a "tight"-structured rhabdovirus nucleocapsid protein.

Rhabdo_ncap (PF00945) is a "tight"-structured rhabdovirus nucleocapsid protein.

VP4_haemagglut (IPR000416) is the concanavalin-like domain of the rotavirus hemagglutinin outer capsid protein VP4. VP4 binds to the sialic acid receptor on the host cell membrane through the viral hemagglutinin, and achieves membrane penetration.

Viral_coat (IPR000937) is the S domain of the capsid protein of a plant icosahedral positive-strand RNA virus. Many S domains are shared by the capsid proteins of numerous plant viruses, including Camovirus, Erhuavirus, Sobemovirus, Tombus virus, and the unidentified tobacco necrosis virus.

Using MEME native tools, we compared Capsid correlations with S or ORF3a, respectively. The S1 subprotein of the S protein contains Adeno_hexon A、Capsid_N A、Gag_p17 A, Pico_P2B A, Rhabdo_ncap A, Rhv A-C domain motifs, as shown in Table 3. The S2 subprotein of the S

protein contains Adeno_hexon B、Adeno_knob A、Calici_coat A, Calici_coat_C A，Capsid_N B，Gag_p17 A, Capsid_NCLDVA-B，Flavi_capsid A-B, Gag_p17 B，Gag_p24 A-B，Gag_p24_C A，HCV_capsid A-B， Hep_core_N A-B, Nepo_coat_C A, Nepo_coat_N A，Parvo_coat A-B, Pico_P2A A, Pico_P2B B-C, Rhabdo_ncap B, Rhv D-F, VP4_haemagglutA-B, Viral_coat A domain motifs.

The capsid-like domain of the S2 protein is primarily located in the cysteine-rich region, and this region and nearby sites are primarily involved in membrane fusion; therefore, the capsid-like domain of the S2 protein is not utilized in the construction of viral vectors. The membrane fusion mechanism of S2 membrane glycoprotein shares an evolutionary relationship with the capsid. Table 3 demonstrates that Adeno hexon A, Capsid NA, Gag p17 A, Rhabdo ncap, and Rhv A overlap in the capsid-like domain of the S1 protein. Rhv A (residues 143–161) is the longest, however. The S protein constructs the virus vector via the Rhv A, Rhv B, and Rhv C domains of the S1 protein, i.e., the picornavirus-like capsid protein activity.

Table 3 demonstrates that ORF3a has more capsid-like active domain motifs, the Rhv A and viral coat A-C motifs being the longest. All of these motifs overlap in the Rhv A region. The viral coat is the S domain of the capsid of plant viruses, which is responsible for viral shell construction. Therefore, ORF3a has capsid protein activity similar to picornaviruses. This activity shares an evolutionary relationship with the S domain of plant virus capsids. Table 3 demonstrates that ORF3a lacks the chitin-binding function of viruses; consequently, ORF3a's capsid protein activity is not used to construct virus vectors. ORF3a disguises itself through the activity of capsid proteins, luring blood or immune cells.

3.3 The Haem_bd domain of viral proteins could bind heme.

The UniProt database was used to find cytochrome C-related sequences. Then we adopted the local version of MEME to match the viral proteins and cytochrome C-related sequences. Due to the large number of motif fragments, we organized motif sequences by protein and domain. Table 4 displays the search results. S, N, E, ORF3a, ORF7b, ORF10, nsp2, nsp3, and RdRP all have Haem_bd domains, as seen in Table 4. A possible heme-binding motif CXXCH can be found in the Haem_bd (PF14376) domain. H connects to the iron in heme, while two Cs bind to porphyrin[117]. The Haem_bd domain is found in most cytochrome C oxidases. It demonstrates that the Haem bd domain of these viral proteins can bind heme.

The Haem_bd domain of S and ORF3a proteins overlaps with its capsid domain. Binding of HEME may inhibit their capsid activity.

Table 4. Haem_bd domain of SARs-CoV-2 viral protein

Protein	Alias	Haem_bd Motif	Start	END
S	A	NFTTAPAICHDGKAHFPRE	1074	1092
	B	GKYEQYIKWPWYIWLGFIAGLIAIVMVTIMLCCM	1204	1237
E	A	RLCAYCC	38	44
N	A	PRWYFYYLGTGPEAGLPYGANKDGIIWVATEGALNTPKDH	106	145
	B	QGTDYKHWPQIAQFAPSASAFFGMSRIGMEVTPSGTWLTY	294	333
	C	VILLNKHIDAYKTFPPTE	350	367
ORF3a	A	NFVRIIMRLWLCWKCRS	119	135
	B	NCYDYC	152	157
ORF7b	A	QDHNETCH	35	42

ORF10	A	CRMNSRNY	19	26
nsp2	A	KRGVYCCREHEHEIAWYTERSEKSYELQTPFE	45	76
nsp3	A	CASEYTGNYQCGHYKHI	1005	1021
RdRP	A	PHLMGWDYPKCDRAMPNMLRIMASLVLARKH	612	642

According to the motif CXXCH of the linked sequences, we formed a one-to-one correlation with the results in Table 4, and then sorted out the Haem motif (Table 5). Only E and ORF3a carry the CXXC motif, as shown in Table 5. Hematoporphyrin binds both C molecules. E has C44 as and Fe binding site, and ORF3a has R134. But neither does H. This mutation may make it easier for viral proteins to bind iron. E and ORF3a bind to heme in a relatively steady manner. Other viral proteins' heme-binding could be unstable as well.

Table 5. The Haem motif of CXXCH is in the SARs-CoV-2 viral protein.

Protein	Alias	Haem motif	Start-End	Haem-Fe Site
S	A	PAICH	1079-1083	H1083
	B	KYEQY	1205-1209	Y1209
E	A	CAYCC	40-44	C44
N	A	WYFYY, YYLGT	108-112, 111-115	Y112, T115
	B	TDYKH, DYKHW	296-300, 297-301	H300, W301
	C	NKHID, HIDAY	354-358, 356-360	D358, Y360
ORF3a	A	CWKCR	130-134	R134
	B	CYDYC	153-157	C157
ORF7b	A	NETCH	38-42	H42
nsp2	A	VYCCR	228-232	R232
nsp3	A	CASEY	1823-1827	Y1827

3.4 Viral proteins could bind hemoglobin

Eryth_link_C is on the linker subunit of the giant extracellular hemoglobin (globin) respiratory complex. The linker subunit's C-terminal globular domain is involved in trimerization. It also interacts with globin and other adjacent trimers' C-terminal spherical linker domains. In Staphylococcus aureus, the NEAT domain encodes the human hemoglobin receptor. The NEAT domain recognizes a subfamily of iron-regulated surface determinant proteins that are found exclusively in bacteria. Iron-regulated surface determining protein H (isdH, also known as harA) interacts with the human plasma haptoglobin-hemoglobin complex, haptoglobin, and hemoglobin. It has a much higher affinity for haptoglobin-hemoglobin complexes than haptoglobin alone. These three domains serve distinct purposes. IsdH(N1) binds hemoglobin and haptoglobin; IsdH(N3) binds heme that has been released from hemoglobin.

We downloaded hemoglobin-related sequences from the UniProt database. We then compared the viral proteins to the hemoglobin-related sequences using the local MEME version. We combined the motif sequence by protein and domain due to the vast number of motif pieces. Table 6 summarizes the search results. S, E, N, ORF3a, ORF6, ORF7a, ORF7b, ORF8, ORF10, 2'-O-ribose methyltransferase contain NEAT domains, as shown in Table 6. The domain Eryth_link_C is present in S, N, ORF6, ORF7b, ORF8, ORF10, nsp6, nsp10, and RdRP. Both Eryth link C and NEAT domains are in S, N, ORF6, ORF7b, ORF8, ORF10, respectively. Because S can form a trimer structure, it can be combined with extracellular hemoglobin. The S Eryth_link_C A is involved in receptor binding. S Eryth_link_C B is a member of the S2 family of

proteins involved in membrane integration. The NEAT domains of S, E, N, ORF3a, ORF6, ORF7a, ORF7b, ORF8, ORF10, and 2'-O-ribose methyltransferase may perform distinct functions. S NEAT A and S Eryth_link_C B are mutually overlapped. E NEAT A is shorter proteins that perform the function of heme capture. S, N, ORF3a, ORF6, ORF7b, ORF8, and ORF10 have a longer NEAT that can bind to and catch hemoglobin.

The hemoglobin domains of the S and ORF3a proteins overlap with their capsid domains. Binding of hemoglobin may inhibit their capsid activity. Thus, viruses evolved the ability to attack hemoglobin.

Table 6. The SARs-CoV-2 virus protein contains the Eryth_link_C and NEAT domains.

Protein	Domain	Alia	Motif	Start	End
S	Eryth_link_C	A	PFLGVYYHKNNKSWMESEFR	139	158
		B	YIKWPWYIWL	1209	1218
	NEAT	A	KWPWYIWLGFIAGLIAIVMVTIMLCCMT	1211	1238
E	Eryth_link_C	A	MYSFVSE	1	7
	NEAT	A	ALRLCAYCCNI	36	46
N	Eryth_link_C	A	YKHWPQIAQF	298	307
	NEAT	A	ELIRQGTDYKHWPQI	290	304
ORF3a	NEAT	A	MRLWLCWKCRSKNPLLYDANYFLCWHTNCYDYCI	125	158
ORF6	Eryth_link_C	A	ILLIIMRTFKVSIWNLDYIINLIIKNLSKSLTENKYSQL DEEQPMEI	14	60
	NEAT	A	ILLIIMRTFKVSIWNLDYIINLIIKN	14	39
ORF7a	NEAT	A	CELYHYQECVR	15	25
ORF7b	Eryth_link_C	A	MLIIFWFSLELQDHNETCH	24	42
	NEAT	A	QDHNETCH	35	42
ORF8	Eryth_link_C	A	AFHQECSLQSCTQHQPYVVDDPCPIHFYSKWYIRVG ARK	15	53
	NEAT	A	HQECSLQSCTQHQPYVVDDPCPIHFYSKWYIRVGA RKSAPLIELCVDEAGSKSPIQYID	17	75
ORF10	Eryth_link_C	A	MGYINVFAFPFTIYSLLLCRMNSRNYIAQVDVVNFN	1	36
	NEAT	A	SLLLCRMNSRNYIAQ	15	29
nsp6	Eryth_link_C	A	FNMVYMPASWVMRIMTW	81	97
nsp10	Eryth_link_C	A	FGGASCCLYCRCHIDH	68	83
RdRP	Eryth_link_C	A	ENPHLMGWDYPKCDRAMPNMLRIM	610	633
2'-O-ribo se methyltra nsferase	NEAT	A	MGHFAWWTAF	184	193

3.5 ORF3a acted as a hemoglobin protease.

The autotransporter subfamily has two peptidase S6 domains (IPR030396 and PS51691). S06.001 - Neisseria type serine peptidase specific for IgA1, MEROPS accession number MER0000278. Peptidase S6 domains are found in the IgA-specific serine endopeptidase autotransporter of Neisseria gonorrhoeae, the immunoglobulin A1 protease autotransporter of Haemophilus influenzae, and the hemoglobin binding protease Hbp autotransporter of pathogenic

Escherichia coli. In contrast to IgA peptidases (Family S6 contains Neisseria and Haemophilus IgA1-specific endopeptidases), Enterobacter sp. (SPATE) peptidases have not been demonstrated to cleave IgA1. SPATE proteins are all highly immunogenic, and each SPATE member is one of the pathogen's most prominent secreted proteins. Human IgA1 is cleaved by the bacterial IgA1 protease at a hinge region where IgA2 is not present. They are highly selective prolyl endopeptidases, and the site of cleavage within human IgA1's hinge region differs between strains. Hbp attaches to hemoglobin, destroys it, and then binds to the heme that is liberated.

His, Asp, Ser, in that order, are the catalytic residues of the S6 family. Ser is found in the Gly-Xaa-Ser-Gly-Xaa-Pro motif, which is highly conserved across the S1-S2 families and the S7, S29, and S30 families. S6 is a member of the PA clan. As established experimentally in the Hap protein of Haemophilus influenza, his and asp residues are positioned around 190 and 120 residues N-terminal to the catalytic Ser. By cleaving human IgA1, the protective role of the powerful medium, IgA1 serine peptidase, may disrupt mucosal surface-specific immunity.

We used a local version of MEM to compare the hemoglobin degrading-related sequences to the SARs-CoV-2 viral protein to identify conserved structures. We combined the motif fragments according to viral protein and domain classification. Table 7 illustrates the domain distribution of Peptidase S6 in SARs-CoV-2. Peptidase S6 domains are shown in Table 7 for E, ORF3a, ORF7a, ORF7b, ORF8, and ORF10. However, only the ORF3a Peptidase S6 domains share a similar Gly-Xaa-Ser-Gly-Xaa-Pro motif: C-R-S-K-N-P. C and K are unambiguously derived from Gly or G. This mutation could be used to improve ORF3a's affinity for heme. As determined by heme motif research, CR is the final two letters of CH in the Haem bind domain's CXXCH motif. C denotes heme's porphyrin-binding site, while R denotes iron-binding. It indicates that ORF3a acts on hemoglobin via the Peptidase S6 domains of the hemoglobin protease. The catalytic site C-R-S-K-N-P acts on the heme on hemoglobin, and then hunts for and binds to heme directly. ORF3a, ORF8, S, and N, as well as others, have a more significant number of autotransporter domains[118]. As a result, ORF3a functioned as an IgA1 peptidase and a hemoglobin protease.

The hemoglobin protease domain of ORF3a protein overlaps with its capsid domain. After hemoglobin binds to the capsid domain of ORF3a protein, ORF3a protein has the ability to attack hemoglobin.

Table 7. The SARs-CoV-2 virus protein contains the Peptidase S6 domain

Domain	Motif	Start	End	X-X-Ser-X-X-Pro
E	CAYCCNIVNVSLVKP	40	54	-
ORF3a	RIIMRLWLCWKCRSKNPLLYDANYFLCWHTNCYDYCIP	122	159	CRSKNP
ORF7a	HPLADNKFALTCFSTQFAFACPDGVKHVY	47	75	-
ORF7b	MIELSLIDFYLCFLAFLLFLVLIMLIIFWFSLELQDHNETCHA	1	43	-
ORF8	PYVVDDPCPIHFYSKWYIRVGARKSAPLI	30	58	-
ORF10	MGYINVFAFPFTIYSLLLCRMNSRNYI	1	27	-

3.6 ORF3a protein possessed IsdA, IsdC, and IsdH activity for uptaking heme.

ORF3a can bind to and degrade hemoglobin, as seen in Tables 6-7. ORF3a can also bind heme, as demonstrated in Tables 4-5. It indicates that ORF3a can bind to and degrade hemoglobin before collecting heme. As seen in Table 6, ORF3a has a NEAT domain. All Isd proteins involved in heme absorption contain NEAT domains. IsdA, IsdC, and IsdH/IsdB proteins are present in

Staphylococcus aureus. They are capable of completing activities such as hemoglobin localization and heme capture. Table 8 summarizes the protein sequences corresponding to the ORF3a's domains are derived from IsdA, IsdC, and IsdH. The three proteins' motifs, notably the heme-binding motif "CWKCR," are remarkably similar, indicating that their functions are intimately tied to heme capture. The searches mentioned above show that the IsdH domain supports ORF3a in localizing hemoglobin, and then the IsdA domain attacks hemoglobin. The IsdA domain is responsible for transferring the heme from hemoglobin to IsdC. IsdC binds to heme.

The Isd domain of ORF3a protein overlaps with its capsid domain. After Hemoglobin alpha chain binds to the capsid domain of ORF3a protein, ORF3a protein has the ability to attack hemoglobin.

Table 8. ORF3a's Isd domains in NEAT domain

Protein	Motif	Start	End
Cell surface protein IsdA, transfers heme from hemoglobin to apo-IsdC	MRLWLCWKCRSKNPLLYDANYFLCW	125	149
Heme uptake protein IsdC	MRLWLCWKCRSKNPLLYDANYFLCWHTNCY DYCI	125	158
Iron-regulated surface determinant protein H (IsdH)	FVRIIMRLWLCWKCR	120	134

3.7 ORF3a protein was capable of converting heme to iron and porphyrin.

The ABM domain (IPR007138) is a monooxygenase domain involved in the biosynthesis of antibiotics. This domain is found in the IsdG and IsdI strains of S. aureus. IsdG and IsdI are heme-degrading enzymes that resemble monooxygenases structurally. This domain is also found in the MhuD heme-degrading monooxygenase from Mycobacterium tuberculosis. HemS/ChuX (IPR007845) is a protein that degrades heme. ABM monooxygenases (IsdG and IsdI) released iron from heme by cleaving the heme tetrapyrrole ring structure in the presence of NADPH cytochrome P450 reductase. HemS catalyzes the release of iron from heme without causing damage to the tetrapyrrole backbone. After HemS binds to heme, the tetrapyrrole ring structure of heme is also broken to release iron in the presence of electron donors such as ascorbate or NADPH-cytochrome P450 reductase.

We retrieved the sequences of proteins involved in heme degradation from the UniProt database. Then we compared them one by one to ORF3a using the local MEME version. We combined the discovered motif fragments according to conserved domains. The heme degradation domains of the ORF3a protein searched are listed in Table 9. ORF3a contains ABM and HemS domains, as shown in Table 9. ORF3a ABM and ORF3a HemS were found to be homologous. The N-terminus of ORF3a ABM includes more "NFVRI" sequence fragments than the N-terminus of ORF3a HemS. The C-terminal region of ORF3a HemS has more "YDYCIPYNS" sequence fragments than the C-terminal region of ORF3a ABM. ORF3a ABM and ORF3a HemS both include the heme-binding motif "CWKCR," indicating that ORF3a ABM and ORF3a HemS can bind heme. As shown in Table 9, the ORF3a protein could directly separate heme into iron and porphyrin via the HemS domain. ORF3a protein could also cleave the tetrapyrrole ring of heme via the ABM/HemS domain, thereby degrading heme and releasing iron in the presence of NADPH-cytochrome P450 reductase.

The heme-degrading domains of ORF3a protein overlaps with its capsid domain. After Heme binds to the capsid domain of ORF3a protein, ORF3a protein has the ability for heme-degrading.

Table 9. ORF3a protein has a heme-degrading domain.

Domain	Motif	Start	End
ABM	NFVRIIMRLWLCWKCRSKNPLLYDANYFLCWHTNC	119	153
HemS	MRLWLCWKCRSKNPLLYDANYFLCWHTNCYDYCIPYNS	125	162

3.8 Released ORF3a protein impaired human respiratory function

We retrieved the crystal structure of ORF3a from the PDB database and then annotated the conserved domains that attack hemoglobin and degrade heme using the Discovery Studio 2016 tool (Figure 1). ORF3a is a dimer in Figure 1. The heme-binding motifs "CWKCR" and "CYDYC" of a monomeric ORF3a are labeled in Figure 1.A. Coincidentally, the two phantoms are positioned adjacent, producing a clip. It indicated that the clip's function was to capture the heme and expel the iron. The NEAT domain of a monomeric ORF3a is labeled in Figure 1.B. The NEAT structure is made up of tightly packed IsdA, IsdC, and IsdH domains. The NEAT domain contains the heme-binding motifs "CWKCR" and "CYDYC". The Peptidase S6 domain of a monomeric ORF3a is labeled in Figure 1.C. The Peptidase S6 domain spans the heme-binding motif "CWKCR" and "CYDYC". These two heme motifs contain the unusual X-X-Ser-X-X-Pro pattern CRSKNP. The Peptidase S6 domain overlaps the NEAT domain. The HemS domain of a monomeric ORF3a is labeled in Figure 1.D. The HemS domain spans the heme-binding motifs "CWKCR" and "CYDYC". The HemS domain overlaps with the NEAT, Peptidase S6, and ABM domains. It implies that the sequence fragments around the heme-binding motifs "CWKCR" and "CYDYC" are highly conserved. They are involved in hemoglobin assault and heme degradation.

ORF3a may have a mechanism for impairing respiratory function. ORF3a infected erythrocytes via domains similar to those found in Plasmodium falciparum. ORF3a formed ion channels by binding to cytoskeletal proteins such as spectrin in red blood cell membranes. In the erythrocyte inner membrane, the HemS, NEAT, Peptidase S6, and ABM domains were located near the cytoplasm. ORF3a interacted with the hemoglobin protein via the NEAT structure. The NEAT domain possessed the IsdA, IsdC, and IsdH functions. If ORF3a might be linked to 1-alpha-Hb via the IsdH domain of the NEAT domain, then the IsdH domain of the NEAT domain would be positioned near the heme-binding region of 1-beta-Hb. ORF3a altered the shape of beta-Hb via the Peptidase S6 domain. As a result, heme was lost from 1-beta-Hb. ORF3a IsdA was responsible for capturing shed heme and transporting it to the region of ORF3a IsdC. Then, via the HemS domain, ORF3a dissociated heme into iron and porphyrin. ORF3a cleaves the tetrapyrrole ring of heme via the HemS or ABM domain in the presence of NADPH-cytochrome P450 reductase to liberate iron. Because ORF3a has Isd domains, hemoglobin that is attacked by ORF3a might keep most of its natural domain but have a reduced ability to transport oxygen.

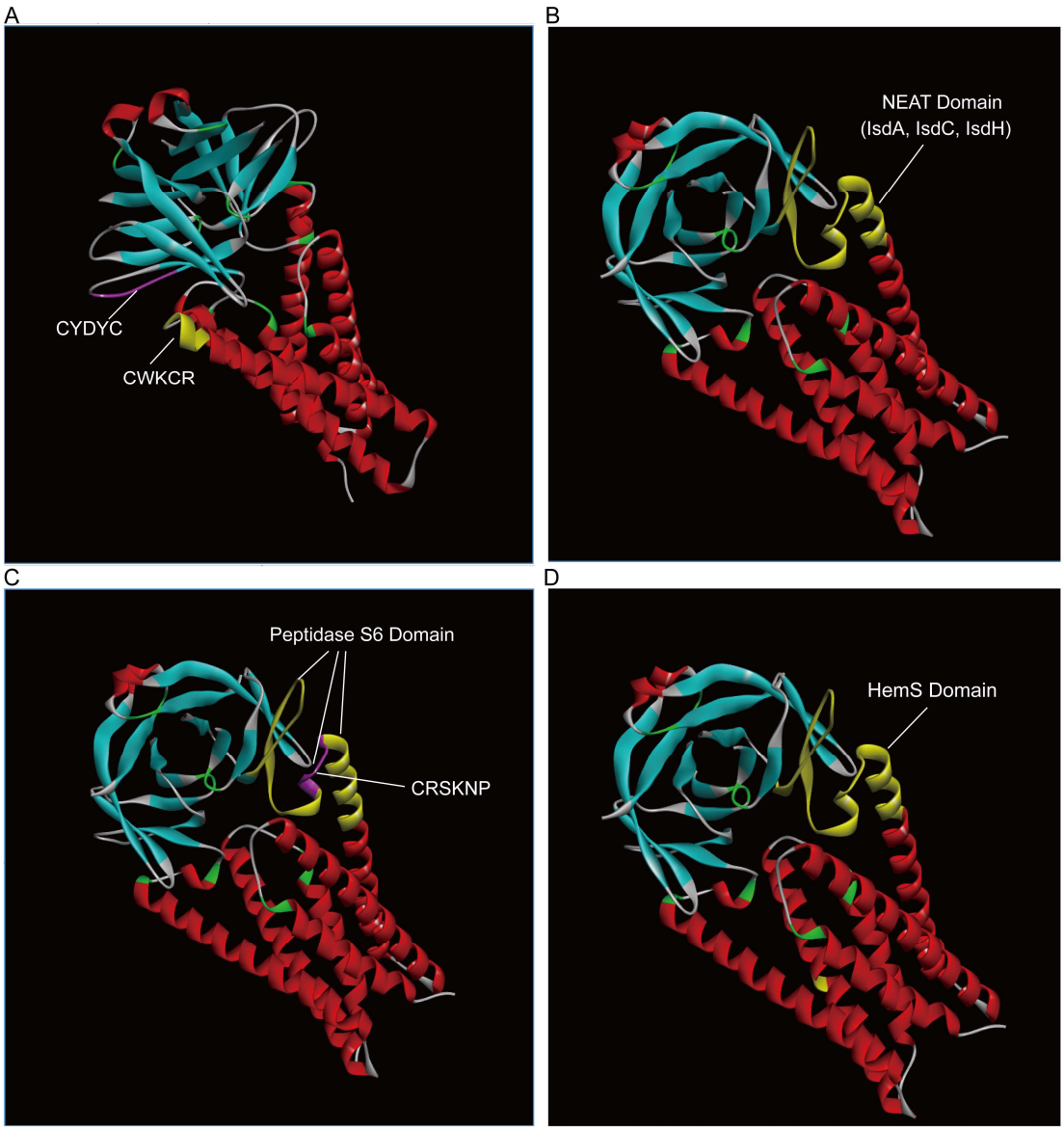

Figure 1. Domains' three-dimensional distribution of ORF3a (PDBID: 6xdc) bound to hemoglobin and cleavage heme. **A.** ORF3a contains two heme-binding motifs. **B.** The ORF3a NEAT domain binds to hemoglobin, including IsdA, IsdC, and IsdH. **C.** ORF3a Peptidase S6 domain catalyzes the degradation of hemoglobin. **D.** ORF3a's HemS domain catalyzes the dissociation of heme into iron and porphyrin. HemS is overlapped with the ABM domain. HemS and ABM split the tetrapyrrole ring of heme and release iron when NADPH-cytochrome P450 reductase is present.

3.9 S protein efficiently transported oxygen molecules through hemocyanin activity

Hemocyanin is commonly found in hexamers and has three copper-binding tyrosinase sites. Because SARs-CoV-2 S protein could form hexamers during membrane fusion, we examined whether S protein possesses hemocyanin activity. We obtained the hemocyanin-related sequences from the Uniprot database and used the local MEME tool to compare them to the S protein individually. Finally, we will combine the searched motifs according to conserved domains. S hemocyanin-related domains are listed in Table 10.

Table 10. Hemocyanin activity-related domains of SARs-CoV-2 S protein

Domain	Alias	Motif	Start	End
Hemocyanin_C	A	EFQFCNDPFLGVYYHKNNKSWME	132	154
	B	RVDFCGKGYHLMS	1039	1051
	C	ICHDGKAH	1081	1088
	D	QELGKYEQYIKWPWYIWLGFIAGLIAIVMVTIMLCCM	1201	1237
Hemocyanin_M	A	WFHAIH	64	69
	B	YYHKNNKSWM	144	153
	C	CTMYICGDSTEC	738	749
	D	FAMQMAYRF	898	906
	E	CHDGKAHFPREG	1082	1093
	F	ELGKYEQYIKWPWYIWLGFIAGLIAIVMVTIMLCCMTS CCSC	1202	1243
Hemocyanin_N	A	KWPWYIWLGFIAGLIAIVMVTIMLCCMTSCC	1211	1241
Tyrosinase_Cu-bd	A	DGKAHFPREG	1084	1093
	B	YEQYIKWPWYIW	1206	1217
	C	CGSC	1250	1253

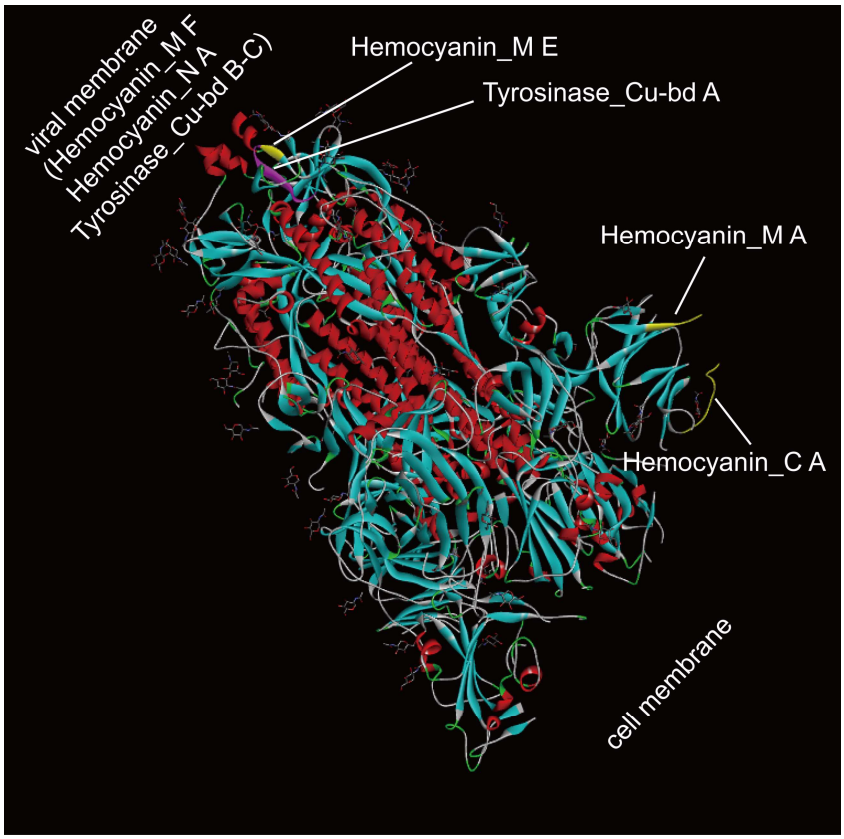

Figure 2. Schematic diagram of the crystal structure positions of the Hemocyanin_M, Hemocyanin_N, Hemocyanin_C, and Tyrosinase_Cu-bd domains of the S protein (PDBID: 6vyb).

According to Table 10, the S protein contains the Hemocyanin protein's C-terminal (Hemocyanin_C), active (Hemocyanin_M), and N-terminal (Hemocyanin_N) domains. The S protein contains three copper-binding tyrosinase regions (Tyrosinase_Cu-bd A-C).

Tyrosinase_Cu-bd A-C are found in the active area of the Hemocyanin protein, Hemocyanin_M domains. Tyrosinase_Cu-bd A resides in Hemocyanin_M E. In contrast, Tyrosinase_Cu-bd B-C resides in Hemocyanin_M F. Hemocyanin_C and Hemocyanin_M are found in the S protein's N to C terminus. Hemocyanin_N is only found at the S protein's C-terminus.

The schematic diagram in Figure 2 illustrates the three-dimensional placements of the domains of Hemocyanin_C, Hemocyanin_M, Hemocyanin_N, and Tyrosinase_Cu-bd. Hemocyanin_N A possesses phenoloxidase activity, but it is located in the transmembrane area. It is consistent with phenol oxidase being isolated from phenolic substrates. Hemocyanin_N also serves as the binding site for the enzyme Tyrosinase_Cu-bd B-C. Tyrosinase_Cu-bd A is located on the exterior of the viral membrane. When Tyrosinase_Cu-bd A binds to Cu, it may initiate a chain reaction, causing a conformational shift in S to expose the Hemocyanin_N domain. Then Tyrosinase Cu-bd B-C binds to copper. After Tyrosinase Cu-bd A-C bind copper, S protein exhibits hemocyanin activity.

Delta (B1.617.2) and Omicron (B.1.1.529) mutants are SARs-CoV-2 viruses that will spread globally starting in 2021. All relevant variants had significantly higher viral loads than the wild type, with Omicron's average viral loads being many times that of Delta[119]. Individuals infected with Omicron exhibit only subtle symptoms. Omicron mutants have a more significant number of mutation sites and a greater capacity for immune evasion. We obtained the ORF3a and S proteins from the NCBI database for the Delta and Omicron mutations. Then, the effects of mutations on the ORF3a and S proteins' attack functions were compared.

3.10 Functional consequences of the Delta and Omicron mutations on the ORF3a and S proteins

Delta (B1.617.2) and Omicron (B.1.1.529) mutants are SARs-CoV-2 viruses that spread globally starting in 2021. All relevant variants had significantly higher viral loads than the wild type, with Omicron's average viral loads being many times that of Delta[119]. Individuals infected with Omicron exhibit only subtle symptoms. Omicron mutants have a more significant number of mutation sites and a greater capacity for immune evasion. We obtained the ORF3a and S proteins from the NCBI database for the Delta and Omicron mutations. Then, the effect of mutations on the ORF3a and S proteins' attack functions was compared.

Mutations in the S protein alleviated symptoms of respiratory distress in patients. We used the local MEME tool to match the S proteins of the Delta and Omicron mutants to hemocyanin-related sequences. The discovered motifs were integrated according to domains, and the resulting search results are displayed in Table 11. The S proteins of Delta and Omicron mutants contain Hemocyanin_C, Hemocyanin_M, Hemocyanin_N, and Tyrosinase_Cu-bd domains, as shown in Table 11. The hemocyanin activity-related domains of the S proteins from SARs2, Delta, and Omicro were mapped using the local version of the IBS tool (Fig. 3).

As illustrated in Figure 3, the S proteins of SARs2, Delta, and Omicro include Hemocyanin C domains in both S1 and S2. As shown in Figure 3, the S protein of SARs2 and Omicro contains the Hemocyanin_N domain. S1 includes the Hemocyanin_N domain of Delta's S protein. As illustrated in Figure 3, the S proteins of SARs2, Delta, and Omicro include Hemocyanin_M domains in both S1 and S2. However, the three viruses had dramatically varied distributions of Tyrosinase_Cu-bd domains. The S protein of Omicro contains only two Tyrosinase_Cu-bd domains. Omicro S Tyrosinase_Cu-bd B is positioned within the Hemocyanin_M domain, but Omicro S Tyrosinase_Cu-bd A is not. SARs2 contains the Tyrosinase_Cu-bd domains entirely

within the N-terminal Hemocyanin_M domain. Delta has the Tyrosinase_Cu-bd domains in C- and N-terminal Hemocyanin _M domains.

Table 11. Hemocyanin activity-related domains of S protein of Delta and Omicron mutants

Protein	Domain	Alias	Motif	Start	End
Delta S	Hemocyanin_C	A	CEFQFCNDPFLGVYYHKNNKSWME	118	141
		B	RVDFCGKGYHLMS	1026	1038
		C	AICHDGKAHFPREGV	1067	1081
	Hemocyanin_M	A	WFHAIH	51	56
		B	VYYHKNNKSWMESEFRVYSSANNCTFEYV SQPFLMD	130	165
		C	CTMYICGDSTEC	725	736
		D	FAMQMAYRF	885	893
		E	CGKGYHLM	1030	1037
		F	APAICHDGKAHFPREGVFVSNGTHWF	1065	1090
	Hemocyanin_N	A	WFHAIH	51	56
	Tyrosinase_Cu-bd	A	WFHAIHV	51	57
		B	YYHKNNKSWME	131	141
		C	DGKAHFPREG	1071	1080
Omicro S	Hemocyanin_C	A	RVDFCGKGYHLMS	1036	1048
		B	ICHDGKAH	1078	1085
		C	RKDGEWVLLSTFLGRSLEVLFQGPGHHHHH HHHSAWSHPQFE	1222	1263
	Hemocyanin_M	A	CEFQFCNDPF	129	138
		B	HKNNKSWM	141	148
		C	CTMYICGDSTEC	735	746
		D	WTFGAGPALQIPFPMQMAYR	883	902
		E	TFLGRSLEVLFQGPGHHHHHHHHHSAWSHP QFEKG	1232	1265
	Hemocyanin_N	A	FQGPGHHHHHHHHSAWSHPQFEK	1242	1264
	Tyrosinase_Cu-bd	A	DGKAHFPREG	1081	1090
		B	GPGHHHHHHHHSAWSHPQFEK	1244	1264

The above distributions suggest that the S of SARs2 S, the Delta S variant, represents the cell agglutination and immune interference activity of the entire sequence. However, since Omicro's S lacks the tyrosinase_Cu-bd domain, cell agglutination and phenoloxidase activity cannot be fully achieved. On the S sequence, the Delta variant exhibits phenoloxidase activity. The copper-binding site of Delta S is highly exposed and readily possesses phenoloxidase activity. SARs2 S has a copper-binding site in the membrane fusion domain, which requires full exposure of SARs S Tyrosinase_Cu-bd A-C and binding to copper to function as a phenoloxidase. Delta S, and Omicro S all lack or lose their phenoloxidase activity. Since SARs2 S, Delta S, and Omicro S all have tyrosinase Cu binding sites, all three S proteins act as oxygen carriers. Due to the easily accessible copper binding site of Delta S1, Delta S has a high oxygen transport capacity. This may explain why Delta patients have higher viral loads and lower levels of respiratory distress than

SARs2 patients. Omicro S developed into a hemocyanin-like protein capable of carrying oxygen molecules but lacking immunological agglutination and phenoloxidase functions. This may explain why Omicro patients experience fewer severe symptoms and no apparent respiratory distress.

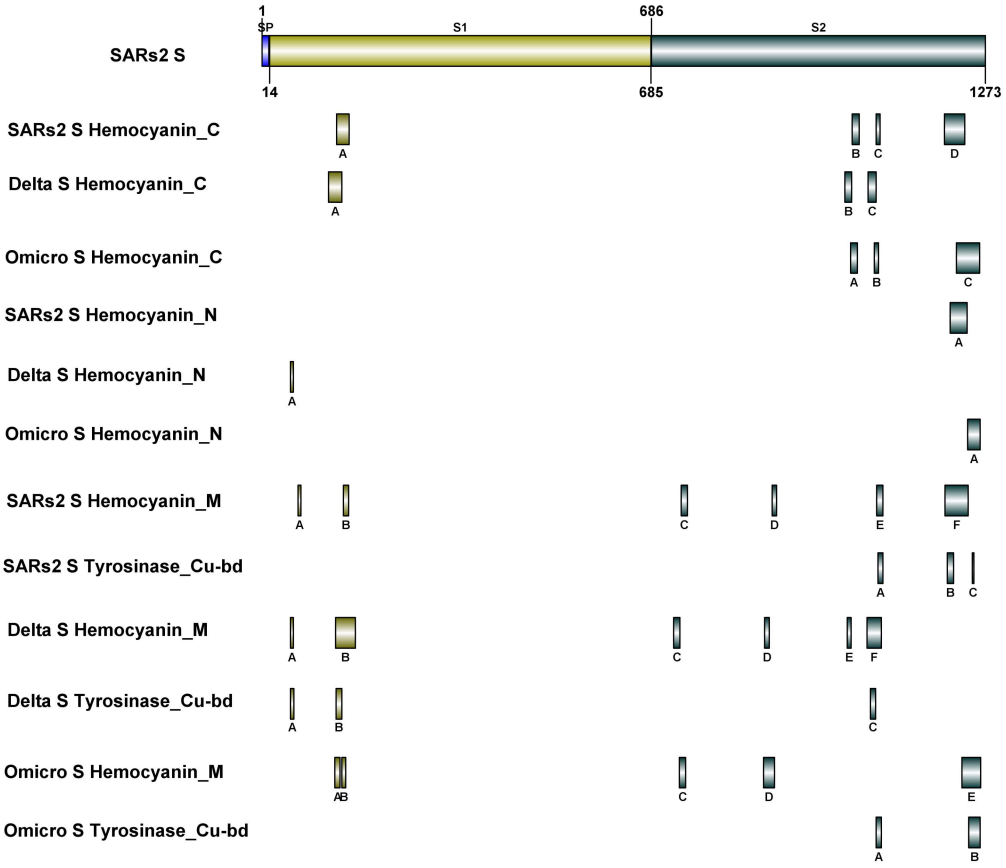

Figure 3. Comparison of hemocyanin activity-related regions of SARs2, Delta, and Omicro S proteins. IBS tools are used to create the diagram[110].

ORF3a mutations had no effect on oxygen supply with reduced hemoglobin. We drew the ORF3a's mutation sites of the hemoglobin attacked-associated domain for SARs2, Delta, and Omicro using a local version of the IBS program (Figure 4). The haeme_bd, NEAT, peptidase S6, IsdA, IsdC and IsdH, ABM, and HemS domains of the SARs2 ORF3a protein are all located within the heme-binding "CWKCR" or "CYDYC" motif, as shown in Figure 4. It suggests that these domains are involved in the degradation, capture, and breakdown of hemoglobin.

Omicro ORF3a does not contain mutations. Delta ORF3a contains two single site mutation 26 and 275. Their mutations are S->L and L->F. Notably, the two Delta ORF3a mutation sites are not located in the Haem_bd, NEAT, peptidase S6, IsdA, IsdC, and IsdH, ABM or HemS domains described above. Therefore, these two point mutations are unlikely to affect ORF3a's hemoglobin attacked, heme capture, or degrade functions.

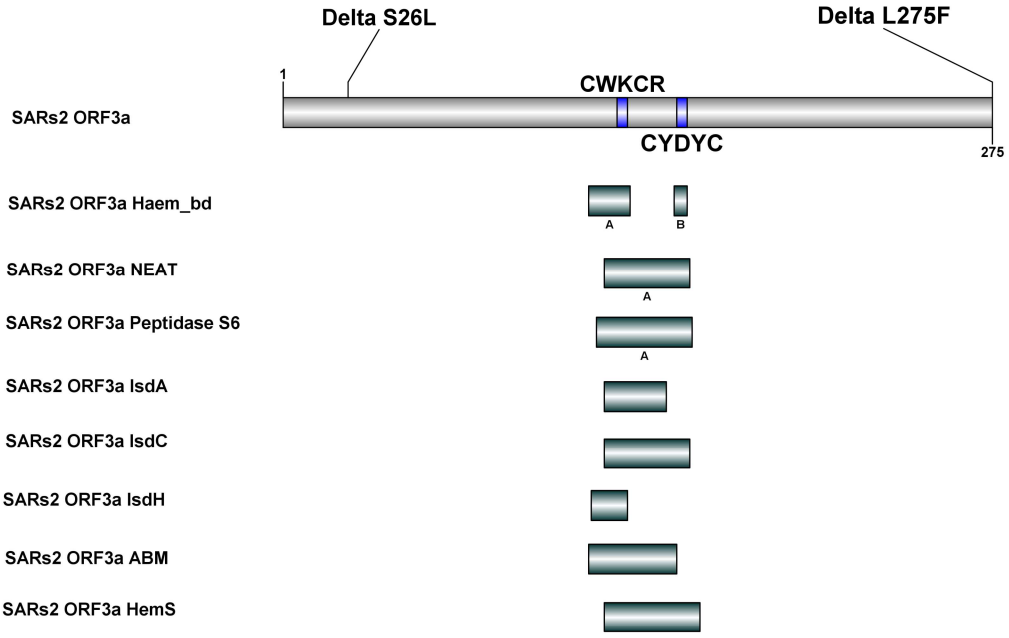

Figure 4. Hemoglobin degradation, heme capture, and disassembly related domains of ORF3a proteins of SARs2, Delta, and Omicro. The figure is drawn with the IBS tool[110].

3.11 How the Capsid-like system of SARs-CoV-2 work

1. S protein inhibits the immune system via the capsid vector.

The S1 protein of the S protein binds chitin via the chitin-binding domain and then uses chitin to adsorb polyphenols. transfer of adsorbed polyphenols to the polyphenol-binding domain of the S1 protein. Fe forms Fe-polyphenol complexes with polyphenols. The FE-polyphenol complex serves as a medium for the SARs-CoV-2 virus to attach the S protein to the red blood cell membrane (marked by the "dashed box" and "Get On" in Figure 5).

SARs-CoV-2 travels to the vicinity of tissue cells by hitching a ride on red blood cells and then release itselef (marked by "Get Off" in Figure 5). Due to the immune delayed effect of this combination and the short transit time, not only is the oxygen-carrying function of red blood cells unaffected, but the immune system cannot detect this cheating behavior.

The wbl domains of the S1 protein is responsible for monitoring nitrosation. If nearby phagocytes are stimulated to release NO, the NO-generated free radicals will attack the S1 protein. Due to the nitration of the wbl domain, the chitin-binding function of the S1 protein was lost (marked by "Nitro-sensing" in Figure 5). S protein oxidizes polyphenols through the action of phenoloxidase, thereby releasing Fe-polyphenol complexes. The SARS-CoV-2 virus escapes immune cell attack and phagocytosis by shedding from red blood cells.

2. Through capsid-like activity, the ORF3a protein stimulates and attacks hemoglobin.

Too many SARs-CoV-2 particles clinging to red blood cells will affect the membrane stability of red blood cells, causing red blood cells to become overloaded. Hemoglobin is released via the enlarged slit in the erythrocyte membrane (marked by "release Hb" in Figure 5). The

released hemoglobin binds NO and then attacks the S protein, damaging the S protein with RNS free radicals.

To protect S protein, ORF3a binds actively to released hemoglobin via a capsid-like activity. And then ORF3a attacks hemoglobin 1-beta chain via hemoglobinase and isd domains. The attack on hemoglobin causes the release of heme (marked "release heme" in Figure 5). Through hemS domains, ORF3a captures heme and decomposes it into iron and porphyrin.The destruction of heme and the attack of ORF3a on hemoglobin will cause damage to the respiratory system. However, the oxygen-transporting ability of the S protein's hemocyanin functional domain can alleviate respiratory dysfunction.

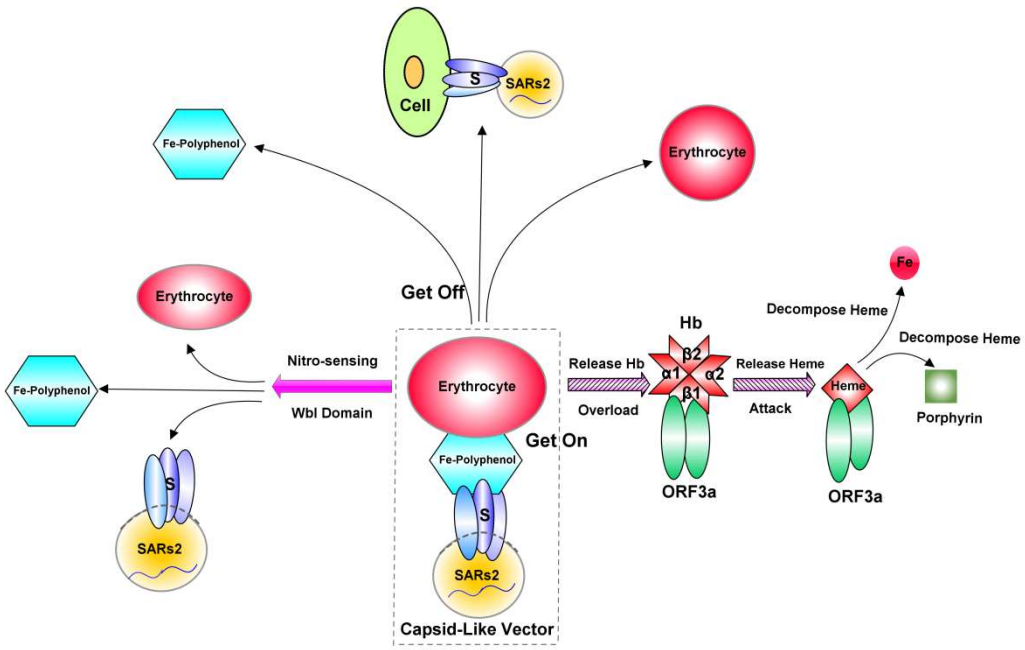

Figure 5. S and ORF3a delay the immune system and damage the respiratory system through the capsid-like system. The figure is drawn with the IBS tool[110].

4 Discussion

4.1 S protein binds porphyrin to cause high viral infection

Non-enveloped viruses are surrounded by a protein capsule, whereas enveloped viruses are surrounded by a lipid bilayer. Both enveloped and non-enveloped virus particles require specific interactions between host cell molecules (or receptors) and envelope (or capsid proteins) encoded by the virus[120]. Most viruses enter cells by endocytosis. Non-enveloped animal viruses require membrane penetration but not membrane fusion to enter cells[121]. HIV and polioviruses are believed to be capable of directly penetrating the plasma membrane of the host cell[120]. Electron microscopy reveals that poliovirus particles are either adjacent to or have directly penetrated the plasma membrane, and that virus particles in the periplasm frequently appear swollen and deformed[122]. There was never any indication of viral entry via pinocytosis[122]. Polioviruses are picornacleic acid (RNA) viruses. According to this study, SARs-CoV-2 S has picornavirus capsid protein activity. SARs-CoV-2 may therefore be capable of directly penetrating the cell membrane.

The HemS protein stimulates the release of iron from heme, leaving behind hematoporphyrin.

Most porphyrin molecules are hydrophobic and agglomerate in water[123]. Porphyrin photosensitizers with a higher hydrophobicity penetrate mammalian cell membranes[124]. Porphyrins diffuse through the phospholipid bilayer and accumulate in the cytoplasm due to concentration gradients[125]. Porphyrin chemicals, such as synthetic photosensitizers, are frequently utilized to treat cancers by photodynamic therapy[126]. Porphyrin derivatives get into cancer cells through endocytosis and concentration gradient osmosis[127]. Porphyrins produce reactive oxygen species (ROS) that kill tumor cells[128].

Medical workers have detected the novel coronavirus from urine, saliva, feces, and blood since the virus can live in body fluids. In such media, the porphyrin is a prevalent substance, and porphyrin compounds are a class of nitrogen-containing polymers. Existing studies have shown that they have a strong ability to locate and penetrate cell membranes. So, the novel coronavirus may also be able to get into human cells directly by using linking porphyrin. The SARs-CoV-2 viral proteins bound porphyrin (or heme) to get energy and cell membrane penetration. It generated reactive oxygen species (ROS) that damage the cell membrane. Porphyrins are mostly preserved in the human body as heme on hemoglobin. The virus's high requirement for porphyrin and iron also developed to attack hemoglobin and break heme into iron and porphyrin.

4.2 Higher hemoglobin causes higher morbidity

The novel coronavirus pneumonia might be closely related to abnormal hemoglobin metabolism in humans. The number of hemoglobin is a significant blood biochemical indicator, and the content varies with gender. The number of normal men is significantly higher than that of normal women, which might also be a reason why men are more likely to be infected with the novel coronavirus pneumonia than women. Besides, most patients with the novel coronavirus pneumonia are the middle-aged and older adults, and many of these patients have underlying diseases such as diabetes. Diabetic patients have higher glycated hemoglobin which is deoxyhemoglobin and is also a combination of hemoglobin and blood glucose, which is another reason for the high infection rate for the elder people. This present study has confirmed that ORF3a could coordinately attack the heme on the beta chain of hemoglobin. Both oxygenated hemoglobin and deoxygenated hemoglobin are attacked by the virus, but the latter is more attacked by the virus. During the attack, the positions of ORF3a are slightly different, which shows that the higher the hemoglobin content, the higher the risk of disease. However, it is not certain that the disease rate incited by abnormal hemoglobin (structural) is relatively low. The hemoglobin of patients and rehabilitees could be detected for further research and treatment.

4.3 Interfering with the normal heme anabolic pathway

This article held that the virus directly interfered with the assembly of human hemoglobin. The main reason was that the normal heme was too low. Heme joins in critical biological activities such as regulation of gene expression and protein translation, and the porphyrin is an essential material for the synthesis of the heme. As the existing traces show there is too much free iron in the bodies of critically ill patients, it could be that the virus-producing molecule competes with iron for the porphyrin, inhibiting the heme anabolic pathway and causing symptoms in humans. It is not clear whether the spatial molecular structure of the heme and porphyrins in patients with porphyria is the same as that in healthy people. If there is an abnormal structure, it is not obvious whether this porphyrin can bind to a viral protein to form a complex, or whether a viral protein can attack this heme. It could be proven by clinical and experimental research.

The disorder of the body's porphyrin metabolism causes Porphyria. Atypical porphyrins have been identified in patients with acquired immunodeficiency syndrome[129]. Chronic hepatic porphyria, not delayed cutaneous porphyria, is the form of porphyrin metabolic illness caused by the hepatitis C virus[129]. Numerous clinical observations have revealed that patients with COVID-19 also have skin and nervous system symptoms consistent with porphyria. Genetic abnormalities in the heme biosynthesis enzyme uroporphyrinogen III synthase also cause congenital erythropoietic porphyria[130]. The SARs-CoV-2 viral protein may has uroporphyrinogen III synthase activity and contribute to infection by producing comparable heme. This type of uroporphyrinogen III synthase inhibited the metabolism of porphyrins.

4.4 Novel coronavirus has a strong carcinogenicity

Numerous published studies demonstrate that after cancer patients get COVID-19, their overall risk of cancer deterioration increases. Numerous clinical studies have established that COVID-19 patients exhibit symptoms consistent with oxidative stress damage. Under conditions of severe oxidative stress, the patient's ROS control mechanism becomes disorganized. The dysregulation of reactive oxygen species (ROS) is a critical element in carcinogenesis. The lungs of the deceased from COVID-19 were mucus-filled, and the deteriorated lung tissue resembled adenocarcinoma-like alterations. During our search for antigen and membrane fusion domains, we discovered that proteins such as S have a melanoma domain . Many malignancies, including lung cancer, have pathogenic proteins that contain melanoma domains. Besides, we were conducting computer research and discovered that proteins such as S contain p53 domains. Normal cells could develop cancer cells when the P53 protein is mutated. We believe that the SARs-CoV-2 virus is highly carcinogenic based on these comprehensive characteristics.

4.5 COVID-19 patients may exhibit quinone poisoning and hyperpigmentation symptoms

Typically, phenols are hydroxylated to catechols and degraded via meta or ortho pathways under aerobic conditions. Tyrosinase oxidizes phenolic substances such as tyrosine and dopamine using molecular oxygen (O2). The presence of catechols results in the formation of benzoquinones. Phenoloxidase converts phenols to quinones. The enzyme phenoloxidase converts phenol to the quinone p-benzoquinone. Benzoquinone is a biochemical with a high irritant potential. After inhalation, it will cause poisoning, resulting in a burning sensation, coughing, shortness of breath, headaches, and other symptoms that cause pain throughout the body. Low-dose idebenone can improve brain function, metabolism, and brain dysfunction; increase the utilization rate of glucose in the brain; and promote ATP production. It can also improve the metabolism of the neurotransmitter 5-hydroxytryptamine in the brain and has powerful antioxidant and free radical-scavenging effects. Benzoquinone, the oxidation product of phenoloxidase of hemocyanin in S protein, caused severe pain in the throat, muscles, and joints of some Omicron patients due in large part to this factor. The benzoquinone content produced by the early version of SARs-CoV-2 S changed rapidly from low to high, and COVID-19 patients rapidly entered a state of benzoquinone poisoning and hypoxia following a brief "happy hypoxia."

Pigmentation also occurs in some pathogen-infected lower species. Hemocyanin's extracellular phenoloxidase (PO) is the primary source of hyperpigmentation (melanosis) in shellfish[131, 132]. Phenoloxidase activity resulting from hemocyanins contributes to brown algal hyperpigmentation. Hemocyanin is the pigment that causes hyperpigmentation in *N. norvegicus*

[133]. However, in COVID-19 patients, an overabundance of synthetic melanin might result in hyperpigmentation.

Colistin B and coronavirus may result in significant skin darkening in patients with COVID-19 who are rescued with ECMO[134]. Dermatological symptoms of COVID-19 include[135]: urticaria, erythema confluent/maculopapular/measles-like rash[136], papular rash, chilblain-like lesions, livedo reticularis/racemoid pattern, and purpura" Vasculitis". The erythema associated with certain severe skin diseases might be converted to hyperpigmentation. Patients with COVID-19 ocular infection develop unilateral acute posterior multifocal lamellar pigment epitheliopathy[137]. COVID-19 patients have bilateral pigmentation of the corneal endothelium, pigment dispersion in the anterior chamber, iris depigmentation with iris transillumination abnormalities[138]. Melanin also has a vital role in the coloration of the oral mucosa[139]. Melanin affects the inflammatory response directly or indirectly by influencing the generation of host cytokines/chemokines[140]. Melanin alters the signaling cascades mediated by cytokines. It boosts the release of pro-inflammatory mediators such as interleukin (IL)-1, IL-6, interferon gamma , and tumor necrosis factor[140].

4.6 Existing blood oxygen detection methods have limitations

If COVID-19 patients had hemoglobin and hemocyanin-like co-transport oxygen patterns, hemocyanin-mediated oxygenation leads to effective O2 transport under hypoxic settings. Oxygen supplied by hemocyanin-like molecules compensates for bodily hypoxia even when red blood cells or hemoglobin were not working adequately. However, the current approach of light absorption in oxygenation detection considered hemoglobin solely and ignored oxygen-carrying hemocyanin-like. Present blood gas detection technologies presupposed that the oxygen molecules in the blood were dissolved oxygen which was not bound to hemoglobin[141]. But the implicit condition that hemocyanin-like could also bind oxygen molecules was ignored. pO_2 determined how much oxygen was bound by hemoglobin and hemocyanin-like proteins. Existing assays overestimated hemoglobin's oxygen supply status. The patient's oxygenation curve may remain unchanged. The actual oxygenation curve should be moved to the right, lowering hemoglobin's affinity for oxygen. Thus, when viruses attacked hemoglobin, it exhibited “high dissolved oxygen”. In contrast, hemocyanin-like proteins exhibited an abnormal oxygen transport function, resulting in "happy hypoxia."

5. Conclusion

Genetic cross-recombination of SARs-CoV-2 viruses in bats, exhibiting similar activities to Flaviviridae, Adenoviridae, Iridoviruses, and Picornaviruses. In this study, the biological functions of SARs-CoV-2 proteins were investigated using bioinformatic techniques involving the search for conserved domains. According to studies, the S and ORF3a proteins of SARs-CoV-2 have capsid domains similar to picornaviruses/caliciviruses and can bind hemoglobin, heme, and porphyrin. Arg134 of ORF3a and Cys44 of E are the sites for heme iron binding. The ORF3a protein contains a domain that converts heme into iron and porphyrin. In addition to chitin-binding and polyphenol-binding domains, the S protein also contains hemocyanin and phenoloxidase-like domains.

S-protein binds chitin in order to absorb polyphenols. Iron ions form Fe-polyphenol complexes with polyphenols. This Fe-polyphenol complex links the S protein and the erythrocyte

membrane, allowing SARs-CoV-2 to ride erythrocytes for rapid delivery to target organs. Due to the delayed immune response, this type of capsid vector enables the virus to achieve rapid immune evasion without significantly altering the oxygen-carrying capacity of red blood cells. Red blood cells loaded with excess virus particles release hemoglobin due to deformation of the cell membrane, and the hemoglobin bound to NO damages the virus via nitration. After the wbl domain of the S protein detects nitration, a conformational change will be induced, and the phenoloxidase domain will oxidize polyphenols, allowing the virus to shed from the red blood cell membrane.

ORF3a also attacks 1-beta chain of hemoglobin to release heme, but the majority of hemoglobin's native structure is preserved. The destruction of hemoglobin and heme by the ORF3a protein causes patients to experience varying degrees of respiratory distress and coagulation, but the hemocyanin-like domain of the S protein can transport oxygen to improve the patient's breathing.

Declarations

Ethics approval and consent to participate

Not applicable.

Consent for publication

Not applicable.

Availability of data and material

The datasets and results supporting the conclusions of this article are available at https://pan.baidu.com/s/1cj4QEHgj-BI0LBo0ulYCJQ, code: skw3.
Or: https://mega.nz/folder/ljpwhSpL#_JnYggFZWM83k73yuxQsXw

Competing interests

The authors declare that they have no competing interests.

Funding

This work was funded by a grant from the Zigong City Key Science and Technology Plan Project (award number: 2021YLSF27, grant recipient: LWZ). This work was partly funded by a grant from the Talent Introduction Project of Sichuan University of Science and Engineering (award number: 2018RCL20, grant recipient: WZL).

Author’s contribution

Funding was obtained by WZL. Besides, design, analysis and writing are finished by WZL, while data curation and manuscript check are undertaken by HLL. Both authors have read and agreed to the published version of the manuscript.

Acknowledgements

Not applicable.

Author details

[1] School of Computer Science and Engineering, Sichuan University of Science & Engineering, Zigong, 643002, China.
[2] School of Life Science and Food Engineering, Yibin University, Yibin, 644000, China.

References

1. Liang W, Feng Z, Rao S, Xiao C, Xue X, Lin Z*, et al.* Diarrhoea may be underestimated: a missing link in 2019 novel coronavirus. *Gut* 2020, **69**(6)**:** 1141-1143.
2. Chan JF-W, Yuan S, Kok K-H, To KK-W, Chu H, Yang J*, et al.* A familial cluster of pneumonia associated with the 2019 novel coronavirus indicating person-to-person transmission: a study of a family cluster. *The lancet* 2020, **395**(10223)**:** 514-523.
3. Hassan SA, Sheikh FN, Jamal S, Ezeh JK, Akhtar A. Coronavirus (COVID-19): a review of clinical features, diagnosis, and treatment. *Cureus* 2020, **12**(3).
4. Lippi G, South AM, Henry BM. Electrolyte imbalances in patients with severe coronavirus disease 2019 (COVID-19). *Annals of clinical biochemistry* 2020, **57**(3)**:** 262-265.
5. Hong X, Xiong J, Feng Z, Shi Y. Extracorporeal membrane oxygenation (ECMO): does it have a role in the treatment of severe COVID-19? *International Journal of Infectious Diseases* 2020, **94:** 78-80.
6. Ñamendys-Silva SA. ECMO for ARDS due to COVID-19. *Heart & Lung: The Journal of Cardiopulmonary and Acute Care* 2020, **49**(4)**:** 348-349.
7. Xia S, Wang L, Zhu Y, Lu L, Jiang S. Origin, virological features, immune evasion and intervention of SARS-CoV-2 Omicron sublineages. *Signal Transduction and Targeted Therapy* 2022, **7**(1)**:** 1-7.
8. Kupferschmidt K. Where did 'weird'Omicron come from? : American Association for the Advancement of Science; 2021.
9. Viana R, Moyo S, Amoako DG. Rapid epidemic expansion of the SARS-CoV-2 Omicron variant in southern Africa. *Nature* 2022, **603**(7902)**:** 679-686.
10. Siow I, Lee KS, Zhang JJY, Saffari SE, Ng A. Encephalitis as a neurological complication of COVID-19: A systematic review and meta-analysis of incidence, outcomes, and predictors. *European Journal of Neurology* 2021, **28**(10)**:** 3491-3502.
11. Costa-Filho RC, Castro-Faria Neto HC, Mengel J, Pelajo-Machado M, Martins MA, Leite ÉT*, et al.* Should COVID-19 be branded to viral thrombotic fever? *Memórias do Instituto Oswaldo Cruz* 2021, **116**.
12. Davis G, Li K, Thankam FG, Wilson DR, Agrawal DK. Ocular transmissibility of COVID-19: possibilities and perspectives. *Molecular and Cellular Biochemistry* 2022**:** 1-16.
13. Faour WH, Choaib A, Issa E, Choueiry FE, Shbaklo K, Alhajj M*, et al.* Mechanisms of COVID-19-induced kidney injury and current pharmacotherapies. *Inflammation Research* 2022, **71**(1)**:** 39-56.
14. Dawood RM, Salum GM, Abd El-Meguid M. The impact of COVID-19 on liver injury. *The American Journal of the Medical Sciences* 2022, **363**(2)**:** 94-103.
15. Zhang Y, Zeng X, Jiao Y, Li Z, Liu Q, Ye J*, et al.* Mechanisms involved in the development of thrombocytopenia in patients with COVID-19. *Thrombosis research* 2020, **193:** 110-115.
16. Budkina AY, Korneenko EV, Kotov IA, Kiselev DA, Artyushin IV, Speranskaya AS*, et al.* Utilizing the VirIdAl Pipeline to Search for Viruses in the Metagenomic Data of Bat Samples. *Viruses*; 2021.
17. Howard CR, Fletcher NF. Emerging virus diseases: can we ever expect the unexpected? *Emerging Microbes & Infections* 2012, **1**(1)**:** 1-9.
18. Enjuanes L, Sola I, Almazan F, Ortego J, Izeta A, Gonzalez JM*, et al.* Coronavirus derived expression systems. *Journal of Biotechnology* 2001, **88**(3)**:** 183-204.

19. de Haan Cornelis AM, Haijema Bert J, Boss D, Heuts Frank WH, Rottier Peter JM. Coronaviruses as Vectors: Stability of Foreign Gene Expression. *Journal of Virology* 2005, **79**(20)**:** 12742-12751.
20. Zhao Z, Pan DC, Qi QM, Kim J, Kapate N, Sun T*, et al.* Engineering of Living Cells with Polyphenol-Functionalized Biologically Active Nanocomplexes. *Advanced Materials* 2020, **32**(49)**:** 2003492.
21. Wang H, Wang C, Zou Y, Hu J, Li Y, Cheng Y. Natural polyphenols in drug delivery systems: Current status and future challenges. *Giant* 2020, **3:** 100022.
22. Zhou J, Lin Z, Ju Y, Rahim MA, Richardson JJ, Caruso F. Polyphenol-Mediated Assembly for Particle Engineering. *Accounts of Chemical Research* 2020, **53**(7)**:** 1269-1278.
23. Zhao Z, Kim J, Suja VC, Kapate N, Gao Y, Guo J*, et al.* Red Blood Cell Anchoring Enables Targeted Transduction and Re-Administration of AAV-Mediated Gene Therapy. *Advanced Science* 2022, **9**(24)**:** 2201293.
24. Park T, Kim JY, Cho H, Moon HC, Kim BJ, Park JH*, et al.* Artificial spores: Immunoprotective nanocoating of red blood cells with supramolecular ferric ion-tannic acid complex. *Polymers* 2017, **9**(4)**:** 140.
25. Guo J, Ping Y, Ejima H, Alt K, Meissner M, Richardson JJ*, et al.* Engineering Multifunctional Capsules through the Assembly of Metal–Phenolic Networks. *Angewandte Chemie International Edition* 2014, **53**(22)**:** 5546-5551.
26. Gu L, Krendelchtchikova V, Krendelchtchikov A, Farrow AL, Derdeyn CA, Matthews QL. Adenoviral vectors elicit humoral immunity against variable loop 2 of clade C HIV-1 gp120 via "Antigen Capsid-Incorporation" strategy. *Virology* 2016, **487:** 75-84.
27. Pigatto G, Lodi A, Finocchio E, Palma MSA, Converti A. Chitin as biosorbent for phenol removal from aqueous solution: Equilibrium, kinetic and thermodynamic studies. *Chemical Engineering and Processing: Process Intensification* 2013, **70:** 131-139.
28. Thomas Carole J, Brown Helen L, Hawes Chris R, Lee Bum Y, Min M-K, King Linda A*, et al.* Localization of a Baculovirus-Induced Chitinase in the Insect Cell Endoplasmic Reticulum. *Journal of Virology* 1998, **72**(12)**:** 10207-10212.
29. Asher DR, Cerny AM, Finberg RW. The erythrocyte viral trap: Transgenic expression of viral receptor on erythrocytes attenuates coxsackievirus B infection. *Proceedings of the National Academy of Sciences* 2005, **102**(36)**:** 12897-12902.
30. Nombela I, Requena-Platek R, Morales-Lange B, Chico V, Puente-Marin S, Ciordia S*, et al.* Rainbow Trout Red Blood Cells Exposed to Viral Hemorrhagic Septicemia Virus Up-Regulate Antigen-Processing Mechanisms and MHC I&II, CD86, and CD83 Antigen-presenting Cell Markers. *Cells*; 2019.
31. Chandran K, Nibert ML. Protease cleavage of reovirus capsid protein μ1/μ1C is blocked by alkyl sulfate detergents, yielding a new type of infectious subvirion particle. *Journal of virology* 1998, **72**(1)**:** 467-475.
32. Du R, Ho B, Ding JL. Rapid reprogramming of haemoglobin structure-function exposes multiple dual-antimicrobial potencies. *The EMBO journal* 2010, **29**(3)**:** 632-642.
33. Li D, Dong H, Li S, Munir M, Chen J, Luo Y*, et al.* Hemoglobin subunit beta interacts with the capsid protein and antagonizes the growth of classical swine fever virus. *Journal of Virology* 2013, **87**(10)**:** 5707-5717.
34. Zhu J, Wang X, Qi R, Tan Y, Li C, Miao Q*, et al.* Hemoglobin subunit beta interacts with the capsid, RdRp and VPg proteins, and antagonizes the replication of rabbit hemorrhagic disease virus. *Veterinary Microbiology* 2021, **259:** 109143.
35. Kabata M, Hase E, Kimura K, Kobayashi Y, Ueno Y, Yoshimune K. Assay of hemoglobin A1c using lectin from Aleuria aurantia. *AMB Express* 2016, **6**(1)**:** 119.

36. Mackow ER, Barnett JW, Chan H, Greenberg HB. The rhesus rotavirus outer capsid protein VP4 functions as a hemagglutinin and is antigenically conserved when expressed by a baculovirus recombinant. *Journal of Virology* 1989, **63**(4)**:** 1661-1668.
37. Joshua HB, Martina C, Ying D, Eleyna M, Alexander S, Lubka TR*, et al.* Heme induces human and mouse platelet activation through C-type-lectin-like receptor-2. *Haematologica* 2020, **106**(2)**:** 626-629.
38. Schmidt WN, Mathahs MM, Zhu Z. Heme and HO-1 inhibition of HCV, HBV, and HIV. *Frontiers in pharmacology* 2012, **3:** 129.
39. Neris RL, Figueiredo CM, Higa LM, Araujo DF, Carvalho CA, Verçoza BR*, et al.* Co-protoporphyrin IX and Sn-protoporphyrin IX inactivate Zika, Chikungunya and other arboviruses by targeting the viral envelope. *Scientific reports* 2018, **8**(1)**:** 1-13.
40. Huang P-Y, Hsiao H-C, Wang S-W, Lo S-F, Lu M-W, Chen L-L. Screening for the Proteins That Can Interact with Grouper Nervous Necrosis Virus Capsid Protein. *Viruses*; 2020.
41. Invernizzi R. Images from the Haematologica Atlas of Hematologic Cytology: parvovirus-induced pure red cell aplasia. *Haematologica* 2022, **107**(7)**:** 1493-1493.
42. Purcell MK, Pearman-Gillman S, Thompson RL, Gregg JL, Hart LM, Winton JR*, et al.* Identification of the major capsid protein of erythrocytic necrosis virus (ENV) and development of quantitative real-time PCR assays for quantification of ENV DNA. *Journal of Veterinary Diagnostic Investigation* 2016, **28**(4)**:** 382-391.
43. Hedrick R, McDowell T, Groff J, Kent M. Another erythrocytic virus from salmonid fish. *Am Fish Soc Fish Health Sect Newsl* 1987, **15**(5).
44. Landolt M, MacMillan J, Patterson M. Detection of an intra-erythrocytic virus in rainbow trout (Salmo gairdneri). *Fish Health News* 1977, **6**(1)**:** 4.
45. Finstad ØW, Dahle MK, Lindholm TH, Nyman IB, Løvoll M, Wallace C*, et al.* Piscine orthoreovirus (PRV) infects Atlantic salmon erythrocytes. *Veterinary research* 2014, **45**(1)**:** 1-13.
46. Yu K, Ti J, Lu X, Pan L, Liu L, Gao Y*, et al.* Novel duck reovirus exhibits pathogenicity to specific pathogen-free chickens by the subcutaneous route. *Scientific Reports* 2021, **11**(1)**:** 11769.
47. Cole A, Morris TJ. A New Iridovirus of Two Species of Terrestrial Isopods, Armadillidium vulgare and Porcellioscaber. *Intervirology* 1980, **14**(1)**:** 21-30.
48. Millet GP, Debevec T. Altitude and COVID-19: Friend or foe? A narrative review. 2021, **8**(24)**:** e14615.
49. Kobayashi M, Kitayama K, Watanabe M, Makino N. The oxygen transport efficiency of arthropod hemocyanins. *Zoological science* 1995, **12**(3)**:** 271-276.
50. Markl J, Decker H. Molecular structure of the arthropod hemocyanins. *Blood and tissue oxygen carriers*. Springer, 1992, pp 325-376.
51. Linzen B, Soeter N, Riggs A, Schneider H-J, Schartau W, Moore M*, et al.* The structure of arthropod hemocyanins. *Science* 1985, **229**(4713)**:** 519-524.
52. Zhao X, Guo L, Zhang Y, Liu Y, Zhang X, Lun J*, et al.* SNPs of hemocyanin C-terminal fragment in shrimp Litopenaeus vannamei. *FEBS letters* 2012, **586**(4)**:** 403-410.
53. Qin Z, Babu VS, Wan Q, Muhammad A, Li J, Lan J*, et al.* Antibacterial activity of hemocyanin from red swamp crayfish (Procambarus clarkii). *Fish & shellfish immunology* 2018, **75:** 391-399.
54. Coates CJ, Decker H. Immunological properties of oxygen-transport proteins: hemoglobin, hemocyanin and hemerythrin. *Cellular and Molecular Life Sciences* 2017, **74**(2)**:** 293-317.
55. Magnus KA, Hazes B, Ton-That H, Bonaventura C, Bonaventura J, Hol WG. Crystallographic analysis of oxygenated and deoxygenated states of arthropod hemocyanin shows unusual differences. *Proteins: Structure, Function, and Bioinformatics* 1994, **19**(4)**:** 302-309.
56. Lutz D. The Many Colors of. *chemmatters* 2010**:** 5.

57. Bux K, Ali SA, Moin ST. Hydration facilitates oxygenation of hemocyanin: perspectives from molecular dynamics simulations. *European Biophysics Journal* 2018, **47**(8)**:** 925-938.
58. Wawrowski A, Matthews PG, Gleixner E, Kiger L, Marden MC, Hankeln T*, et al.* Characterization of the hemoglobin of the backswimmer Anisops deanei (Hemiptera). *Insect biochemistry and molecular biology* 2012, **42**(9)**:** 603-609.
59. Terwilliger NB. Oxygen transport proteins in Crustacea: hemocyanin and hemoglobin. *Physiology* 2015, **4:** 359-390.
60. Pick C, Hagner-Holler S, Burmester T. Molecular characterization of hemocyanin and hexamerin from the firebrat Thermobia domestica (Zygentoma). *Insect biochemistry and molecular biology* 2008, **38**(11)**:** 977-983.
61. Flachsbarth S, Kruse M, Burmester T. Distribution and hypoxia-regulation of haemocyanin in springtails (Collembola). *Insect molecular biology* 2017, **26**(5)**:** 633-641.
62. Chen B, Ma R, Ding D, Wei L, Kang L. Aerobic respiration by haemocyanin in the embryo of the migratory locust. *Insect molecular biology* 2017, **26**(4)**:** 461-468.
63. Lehtonen MP, Burnett LE. Effects of hypoxia and hypercapnic hypoxia on oxygen transport and acid–base status in the Atlantic blue crab, Callinectes sapidus, during exercise. *Journal of Experimental Zoology Part A: Ecological Genetics and Physiology* 2016, **325**(9)**:** 598-609.
64. Head J. The effects of hypoxia on hemocyanin regulation in Cancer magister: Possible role of Hypoxia-Inducible Factor-1. *Journal of experimental marine biology and ecology* 2010, **386**(1-2)**:** 77-85.
65. McMahon BR. Respiratory and circulatory compensation to hypoxia in crustaceans. *Respiration physiology* 2001, **128**(3)**:** 349-364.
66. Decker H, Tuczek F. Tyrosinase/catecholoxidase activity of hemocyanins: structural basis and molecular mechanism. *Trends in biochemical sciences* 2000, **25**(8)**:** 392-397.
67. Cerenius L, Söderhäll K. The prophenoloxidase-activating system in invertebrates. *Immunological reviews* 2004, **198**(1)**:** 116-126.
68. Martínez-Alvarez O, Gómez-Guillén C, Montero P. Presence of hemocyanin with diphenoloxidase activity in deepwater pink shrimp (Parapenaeus longirostris) post mortem. *Food chemistry* 2008, **107**(4)**:** 1450-1460.
69. Lu A, Zhang Q, Zhang J, Yang B, Wu K, Xie W*, et al.* Insect prophenoloxidase: the view beyond immunity. *Frontiers in Physiology* 2014, **5**.
70. Nellaiappan K, Valivittan K. Differentiation of Tyrosine Hydroxylase and Phenol Oxidase after Electrophoresis. *Biotechnic & Histochemistry* 1993, **68**(5)**:** 281-283.
71. Omiadze NT, McHedlishvili NI, Abutidze MO. Phenoloxidases of perennial plants: Hydroxylase activity, isolation and physiological role. *Annals of Agrarian Science* 2018, **16**(2)**:** 196-200.
72. Casey Jr JP. Capsid catalysis: de novo enzymes on viral proteins. Massachusetts Institute of Technology, 2015.
73. Zeng R, Yang R-F, Shi M-D, Jiang M-R, Xie Y-H, Ruan H-Q*, et al.* Characterization of the 3a Protein of SARS-associated Coronavirus in Infected Vero E6 Cells and SARS Patients. *Journal of Molecular Biology* 2004, **341**(1)**:** 271-279.
74. Issa E, Merhi G, Panossian B, Salloum T, Tokajian S. SARS-CoV-2 and ORF3a: Nonsynonymous Mutations, Functional Domains, and Viral Pathogenesis. *mSystems* 2020, **5**(3)**:** e00266-00220.
75. Zhang J, Ejikemeuwa A, Gerzanich V, Nasr M, Tang Q, Simard JM*, et al.* Understanding the Role of SARS-CoV-2 ORF3a in Viral Pathogenesis and COVID-19. *Frontiers in Microbiology* 2022, **13**.
76. Wu S, Tian C, Liu P, Guo D, Zheng W, Huang X*, et al.* Effects of SARS-CoV-2 mutations on protein structures and intraviral protein–protein interactions. *Journal of Medical Virology* 2021, **93**(4)**:** 2132-2140.

77. Bianchi M, Borsetti A, Ciccozzi M, Pascarella S. SARS-Cov-2 ORF3a: mutability and function. *International journal of biological macromolecules* 2021, **170:** 820-826.
78. Gupta S, Mallick D, Banerjee K, Mukherjee S, Sarkar S, Lee STM*, et al.* D155Y substitution of SARS-CoV-2 ORF3a weakens binding with Caveolin-1. *Computational and Structural Biotechnology Journal* 2022, **20:** 766-778.
79. Ertl HCJ. T Cell-Mediated Immune Responses to AAV and AAV Vectors. *Frontiers in Immunology* 2021, **12**.
80. Chen D, Zheng Q, Sun L, Ji M, Li Y, Deng H*, et al.* ORF3a of SARS-CoV-2 promotes lysosomal exocytosis-mediated viral egress. *Developmental Cell* 2021, **56**(23)**:** 3250-3263. e3255.
81. Labadie T, Roy P. A non-enveloped arbovirus released in lysosome-derived extracellular vesicles induces super-infection exclusion. *PLOS Pathogens* 2020, **16**(10)**:** e1009015.
82. Wang R, Yang X, Chang M, Xue Z, Wang W, Bai L*, et al.* ORF3a protein of severe acute respiratory syndrome coronavirus 2 inhibits interferon-activated janus kinase/signal transducer and activator of transcription signaling via elevating suppressor of cytokine signaling 1. *Frontiers in Microbiology* 2021**:** 2871.
83. Airo AM, Felix-Lopez A, Mancinelli V, Evseev D, Lopez-Orozco J, Shire K*, et al.* Flavivirus Capsid Proteins Inhibit the Interferon Response. *Viruses* 2022, **14**(5)**:** 968.
84. Kakkanas A, Karamichali E, Koufogeorgou EI, Kotsakis SD, Georgopoulou U, Foka P. Targeting the YXXΦ Motifs of the SARS Coronaviruses 1 and 2 ORF3a Peptides by In Silico Analysis to Predict Novel Virus—Host Interactions. *Biomolecules* 2022, **12**(8)**:** 1052.
85. Cooper A, Shaul Y. Clathrin-mediated Endocytosis and Lysosomal Cleavage of Hepatitis B Virus Capsid-like Core Particles *. *Journal of Biological Chemistry* 2006, **281**(24)**:** 16563-16569.
86. Karamichali E, Serti E, Gianneli A, Papaefthymiou A, Kakkanas A, Foka P*, et al.* The unexpected function of a highly conserved YXXΦ motif in HCV core protein. *Infection, Genetics and Evolution* 2017, **54:** 251-262.
87. Noor F, Ashfaq UA, Asif M, Adeel MM, Alshammari A, Alharbi M. Comprehensive computational analysis reveals YXXΦ[I/L/M/F/V] motif and YXXΦ-like tetrapeptides across HFRS causing Hantaviruses and their association with viral pathogenesis and host immune regulation. *Frontiers in Immunology* 2022, **13**.
88. Neveu G, Barouch-Bentov R, Ziv-Av A, Gerber D, Jacob Y, Einav S. Identification and Targeting of an Interaction between a Tyrosine Motif within Hepatitis C Virus Core Protein and AP2M1 Essential for Viral Assembly. *PLOS Pathogens* 2012, **8**(8)**:** e1002845.
89. Klein Kevin C, Polyak Stephen J, Lingappa Jaisri R. Unique Features of Hepatitis C Virus Capsid Formation Revealed by De Novo Cell-Free Assembly. *Journal of Virology* 2004, **78**(17)**:** 9257-9269.
90. Stephanopoulos N, Tong GJ, Hsiao SC, Francis MB. Dual-Surface Modified Virus Capsids for Targeted Delivery of Photodynamic Agents to Cancer Cells. *ACS Nano* 2010, **4**(10)**:** 6014-6020.
91. Prasuhn DE, Kuzelka J, Strable E, Udit AK, Cho S-H, Lander GC*, et al.* Polyvalent Display of Heme on Hepatitis B Virus Capsid Protein through Coordination to Hexahistidine Tags. *Chemistry & Biology* 2008, **15**(5)**:** 513-519.
92. Otto BR, van Dooren SJ, Nuijens JH, Luirink J, Oudega B. Characterization of a hemoglobin protease secreted by the pathogenic Escherichia coli strain EB1. *The Journal of experimental medicine* 1998, **188**(6)**:** 1091-1103.
93. Sabotič J, Kos J. Microbial and fungal protease inhibitors—current and potential applications. *Applied Microbiology and Biotechnology* 2012, **93**(4)**:** 1351-1375.
94. Otto BR, Sijbrandi R, Luirink J, Oudega B, Heddle JG, Mizutani K*, et al.* Crystal structure of hemoglobin protease, a heme binding autotransporter protein from pathogenic Escherichia coli. *The Journal of biological chemistry* 2005, **280**(17)**:** 17339-17345.

95. Zhu H, Xie G, Liu M, Olson JS, Fabian M, Dooley DM*, et al.* Pathway for heme uptake from human methemoglobin by the iron-regulated surface determinants system of Staphylococcus aureus. *Journal of biological chemistry* 2008, **283**(26)**:** 18450-18460.
96. Pilpa RM, Robson SA, Villareal VA, Wong ML, Phillips M, Clubb RT. Functionally distinct NEAT (NEAr Transporter) domains within the Staphylococcus aureus IsdH/HarA protein extract heme from methemoglobin. *Journal of Biological Chemistry* 2009, **284**(2)**:** 1166-1176.
97. Krishna Kumar K, Jacques DA, Pishchany G, Caradoc-Davies T, Spirig T, Malmirchegini GR*, et al.* Structural Basis for Hemoglobin Capture by Staphylococcus aureus Cell-surface Protein, IsdH. *Journal of Biological Chemistry* 2011, **286**(44)**:** 38439-38447.
98. Krishna Kumar K, Dickson CF, Weiss MJ, Mackay JP, Gell DA. AHSP (α-haemoglobin-stabilizing protein) stabilizes apo-α-haemoglobin in a partially folded state. *Biochemical Journal* 2010, **432**(2)**:** 275-282.
99. Villareal VA, Pilpa RM, Robson SA, Fadeev EA, Clubb RT. The IsdC protein from Staphylococcus aureus uses a flexible binding pocket to capture heme. *The Journal of biological chemistry* 2008, **283**(46)**:** 31591-31600.
100. Sharp KH, Schneider S, Cockayne A, Paoli M. Crystal structure of the heme-IsdC complex, the central conduit of the Isd iron/heme uptake system in Staphylococcus aureus. *Journal of Biological Chemistry* 2007, **282**(14)**:** 10625-10631.
101. Hurd AF, Garcia-Lara J, Rauter Y, Cartron M, Mohamed R, Foster SJ. The iron-regulated surface proteins IsdA, IsdB, and IsdH are not required for heme iron utilization in Staphylococcus aureus. *FEMS Microbiology Letters* 2012, **329**(1)**:** 93-100.
102. Anzaldi LL, Skaar EP. Overcoming the heme paradox: heme toxicity and tolerance in bacterial pathogens. *Infection and immunity* 2010, **78**(12)**:** 4977-4989.
103. Wilks A, Schmitt MP. Expression and Characterization of a Heme Oxygenase (Hmu O) fromCorynebacterium diphtheriae: IRON ACQUISITION REQUIRES OXIDATIVE CLEAVAGE OF THE HEME MACROCYCLE. *Journal of Biological Chemistry* 1998, **273**(2)**:** 837-841.
104. Skaar EP, Gaspar AH, Schneewind O. IsdG and IsdI, heme-degrading enzymes in the cytoplasm of Staphylococcus aureus. *The Journal of biological chemistry* 2004, **279**(1)**:** 436-443.
105. Létoffé S, Heuck G, Delepelaire P, Lange N, Wandersman C. Bacteria capture iron from heme by keeping tetrapyrrol skeleton intact. *Proceedings of the National Academy of Sciences* 2009, **106**(28)**:** 11719-11724.
106. Stojiljkovic I, Hantke K. Transport of haemin across the cytoplasmic membrane through a haemin-specific periplasmic binding-protein-dependent transport system in Yersinia enterocolitica. *Molecular microbiology* 1994, **13**(4)**:** 719-732.
107. Suits MD, Pal GP, Nakatsu K, Matte A, Cygler M, Jia Z. Identification of an Escherichia coli O157: H7 heme oxygenase with tandem functional repeats. *Proceedings of the National Academy of Sciences* 2005, **102**(47)**:** 16955-16960.
108. Liu M, Boulouis H-J, Biville F. Heme Degrading Protein HemS Is Involved in Oxidative Stress Response of Bartonella henselae. *PLoS One* 2012, **7**(5)**:** e37630.
109. Bailey TL, Johnson J, Grant CE, Noble WS. The MEME suite. *Nucleic acids research* 2015, **43**(W1)**:** W39-W49.
110. Liu W, Xie Y, Ma J, Luo X, Nie P, Zuo Z*, et al.* IBS: an illustrator for the presentation and visualization of biological sequences. *Bioinformatics* 2015, **31**(20)**:** 3359-3361.
111. Wolhuter K, Whitwell HJ, Switzer CH, Burgoyne JR, Timms JF, Eaton P. Evidence against Stable Protein S-Nitrosylation as a Widespread Mechanism of Post-translational Regulation. *Molecular Cell* 2018, **69**(3)**:** 438-450.e435.

112. Chassaing M, Bastin G, Robin M, Majou D, Belliot G, de Rougemont A*, et al.* Free Chlorine and Peroxynitrite Alter the Capsid Structure of Human Norovirus GII.4 and Its Capacity to Bind Histo-Blood Group Antigens. *Frontiers in Microbiology* 2021, **12**.
113. Kudhair BK, Hounslow AM, Rolfe MD, Crack JC, Hunt DM, Buxton RS*, et al.* Structure of a Wbl protein and implications for NO sensing by M. tuberculosis. *Nature Communications* 2017, **8**(1)**:** 2280.
114. Smith LJ, Stapleton MR, Buxton RS, Green J. Structure-function relationships of the Mycobacterium tuberculosis transcription factor WhiB1. *PLoS One* 2012, **7**(7)**:** e40407.
115. den Hengst CD, Buttner MJ. Redox control in actinobacteria. *Biochimica et Biophysica Acta (BBA) - General Subjects* 2008, **1780**(11)**:** 1201-1216.
116. Townsley PM. Chromatography of Tobacco Mosaic Virus (TMV) on Chitin Columns. *Nature* 1961, **191**(4788)**:** 626-626.
117. Babbitt SE, Hsu J, Mendez DL, Kranz RG. Biosynthesis of single thioether c-type cytochromes provides insight into mechanisms intrinsic to holocytochrome c synthase (HCCS). *Biochemistry* 2017, **56**(26)**:** 3337-3346.
118. Liu W, Li H. COVID-19: Invades Erythrocytes through Plasmodium Falciparum Antigen and Complement-Like System. *ChemRxiv Preprint* 2021.
119. Torjesen I. Covid-19: Peak of viral shedding is later with omicron variant, Japanese data suggest. British Medical Journal Publishing Group; 2022.
120. Thorley JA, McKeating JA, Rappoport JZ. Mechanisms of viral entry: sneaking in the front door. *Protoplasma* 2010, **244**(1)**:** 15-24.
121. Liemann S, Chandran K, Baker TS, Nibert ML, Harrison SC. Structure of the Reovirus Membrane-Penetration Protein, μ1, in a Complex with Its Protector Protein, σ3. *Cell* 2002, **108**(2)**:** 283-295.
122. Dunnebacke TH, Levinthal J, Williams RC. Entry and release of poliovirus as observed by electron microscopy of cultured cells. *Journal of virology* 1969, **4**(4)**:** 505-513.
123. Rabiee M, Rabiee N, Salarian R, Rabiee G. Porphyrin-based nanomaterials. *Introduction to Nanomaterials in Medicine*. Morgan & Claypool Publishers, 2019, pp 6-1-6-24.
124. Sułek A, Pucelik B, Kobielusz M, Barzowska A, Dąbrowski JM. Photodynamic Inactivation of Bacteria with Porphyrin Derivatives: Effect of Charge, Lipophilicity, ROS Generation, and Cellular Uptake on Their Biological Activity In Vitro. *Int J Mol Sci* 2020, **21**(22)**:** 8716.
125. Tsubone TM, Martins WK, Pavani C, Junqueira HC, Itri R, Baptista MS. Enhanced efficiency of cell death by lysosome-specific photodamage. 2017, **7**(1)**:** 6734.
126. Kolarova H, Nevrelova P, Tomankova K, Kolar P, Bajgar R, Mosinger J. Production of reactive oxygen species after photodynamic therapy by porphyrin sensitizers. *General physiology and biophysics* 2008, **27**(2)**:** 101-105.
127. Nishida K, Tojo T, Kondo T, Yuasa M. Evaluation of the correlation between porphyrin accumulation in cancer cells and functional positions for application as a drug carrier. *Scientific Reports* 2021, **11**(1)**:** 2046.
128. Clichici S, Filip A, Daicoviciu D, Ion RM, Mocan T, Tatomir C*, et al.* The dynamics of reactive oxygen species in photodynamic therapy with tetra sulfophenyl-porphyrin. *Acta physiologica Hungarica* 2010, **97**(1)**:** 41-51.
129. Gomi H, Hatanaka K, Miura T, Matsuo I. Type of Impaired Porphyrin Metabolism Caused by Hepatitis C Virus Is Not Porphyria Cutanea Tarda but Chronic Hepatic Porphyria. *Archives of Dermatology* 1997, **133**(9)**:** 1170-1171.

130. Romeo G, Levin EY. Uroporphyrinogen 3 cosynthetase in human congenital erythropoietic porphyria. *Proceedings of the National Academy of Sciences of the United States of America* 1969, **63**(3)**:** 856-863.
131. Adachi K, Hirata T, Nagai K, Sakaguchi M. Hemocyanin a most likely inducer of black spots in kuruma prawn Penaeus japonicus during storage. *Journal of Food Science* 2001, **66**(8)**:** 1130-1136.
132. García-Carreño FL, Cota K, Navarrete Del Toro MA. Phenoloxidase activity of hemocyanin in whiteleg shrimp Penaeus vannamei: conversion, characterization of catalytic properties, and role in postmortem melanosis. *Journal of Agricultural and Food Chemistry* 2008, **56**(15)**:** 6454-6459.
133. Coates CJ, Nairn J. Hemocyanin-derived phenoloxidase activity: a contributing factor to hyperpigmentation in Nephrops norvegicus. *Food chemistry* 2013, **140**(1-2)**:** 361-369.
134. Lu C, Hou N. Skin Hyperpigmentation in Coronavirus Disease 2019 Patients: Is Polymyxin B the Culprit? *Frontiers in Pharmacology* 2020, **11**(1304).
135. Genovese G, Moltrasio C, Berti E, Marzano AV. Skin manifestations associated with COVID-19: current knowledge and future perspectives. *Dermatology* 2021**:** 1-12.
136. Recalcati S. Cutaneous manifestations in COVID-19: a first perspective. *J Eur Acad Dermatol Venereol* 2020, **34**(5).
137. Olguín-Manríquez F, Cernichiaro-Espinosa L, Olguín-Manríquez A, Manríquez-Arias R, Flores-Villalobos EO, Kawakami-Campos PA. Unilateral acute posterior multifocal placoid pigment epitheliopathy in a convalescent COVID-19 patient. *International journal of retina and vitreous* 2021, **7**(1)**:** 41.
138. Yagci BA, Atas F, Kaya M, Arikan G. COVID-19 Associated Bilateral Acute Iris Transillumination. *Ocular immunology and inflammation* 2021, **29**(4)**:** 719-721.
139. Iozumi K, Hoganson GE, Pennella R, Everett MA, Fuller BB. Role of tyrosinase as the determinant of pigmentation in cultured human melanocytes. *Journal of Investigative Dermatology* 1993, **100**(6)**:** 806-811.
140. Sidiropoulou P, Docea AO, Nikolaou V, Katsarou M-S, Spandidos DA, Tsatsakis A*, et al.* Unraveling the roles of vitamin D status and melanin during Covid-19 (Review). *Int J Mol Med* 2021, **47**(1)**:** 92-100.
141. Higgins C. Oxygen saturation–better measured than calculated. 2014.